

Quantum heat engines and refrigerators: Continuous devices

Ronnie Kosloff, Amikam Levy

Institute of Chemistry, the Hebrew University, Jerusalem 91904, Israel

Quantum thermodynamics supplies a consistent description of quantum heat engines and refrigerators up to the level of a single few level system coupled to the environment. Once the environment is split into three; a hot, cold and work reservoirs a heat engine can operate. The device converts the positive gain into power; where the gain is obtained from population inversion between the components of the device. Reversing the operation transforms the device into a quantum refrigerator. The quantum tricycle, a device connected by three external leads to three heat reservoirs is used as a template for engines and refrigerators. The equation of motion for the heat currents and power can be derived from first principle. Only a global description of the coupling of the device to the reservoirs is consistent with the first and second laws of thermodynamics. Optimisation of the devices leads to a balanced set of parameters where the couplings to the three reservoirs are of the same order and the external driving field is in resonance. When analysing refrigerators special attention is devoted to a dynamical version of the third law of thermodynamics. Bounds on the rate of cooling when $T_c \rightarrow 0$ are obtained by optimising the cooling current. All refrigerators as $T_c \rightarrow 0$ show universal behavior. The dynamical version of the third law imposes restrictions on the scaling as $T_c \rightarrow 0$ of the relaxation rate γ_c and heat capacity c_V of the cold bath.

Contents

I. Introduction	3
II. The continuous engine	4
A. The quantum 3 level system as a heat engine	5
B. The quantum tricycle	6
C. The quantum amplifier	10
1. Solving the equations of motion for the engine	13
2. Optimizing the amplifier's performance	17
D. Dynamical model of a 3-level engine	18
1. The Generalized Lamb Equations in the P Representation	21
E. The four-level engine and two-level engine	23
F. Power storage	25
III. Continuous refrigerators	26
A. The third law of thermodynamics	26
B. The quantum power driven refrigerator	28
C. Dynamical refrigerator models	29
D. The quantum absorption refrigerator	30
1. The 3-level absorption refrigerator	31
2. Tricycle absorption refrigerator	31
3. Noise driven refrigerator	33
E. Refrigerators operating close to the limit $T_c \rightarrow 0$ and the third-law of thermodynamics	37
IV. Summary	39
References	43

I. INTRODUCTION

Our cars, refrigerators, air-conditioners, lasers and power plants are all examples of heat engines. The trend toward miniaturisation has not skipped the realm of heat engines leading to devices on the nano or even on the atomic scale. Typically, in the practical world all such devices operate far from the maximum efficiency conditions set by Carnot [1]. Real heat engines are optimised for powers sacrificing efficiency. This trade-off between efficiency and power is the focus of "finite time thermodynamics". The field was initiated by the seminal paper of Curzon and Ahlborn [2]. From everyday experience the irreversible phenomena that limits the optimal performance of engines can be identified as losses due to friction, heat leaks, and heat transport [3]. Is there a unifying fundamental explanation for these losses? Is it possible to trace the origin of these phenomena to quantum mechanics? To address these issues the tradition of thermodynamics is followed by the study of hypothetical quantum heat engines and refrigerators. Once understood, these models serve as a template for real devices.

Gedanken heat engines are an integral part of thermodynamical theory. Carnot in 1824 set the stage by analysing an ideal engine [1]. Carnot's analysis preceded the systematic formulation that led to the first and second laws of thermodynamics [4]. Amazingly, thermodynamics was able to keep its independent status despite the development of parallel theories dealing with the same subject matter. Quantum mechanics overlaps thermodynamics in that it describes the state of matter. However, in addition, quantum mechanics include a comprehensive description of dynamics. This suggests that quantum mechanics can originate a concrete interpretation of the word *dynamics* in thermodynamics leading to a fundamental basis for finite time thermodynamics.

Quantum thermodynamics is the study of thermodynamical processes within the context of quantum dynamics. Historically, consistency with thermodynamics led to Planck's law, the basics of quantum theory. Following the ideas of Planck on black body radiation, Einstein in (1905) quantized the electromagnetic field [5]. This paper of Einstein is the birth of quantum mechanics together with quantum thermodynamics.

Quantum thermodynamics is devoted to unraveling the intimate connection between the laws of thermodynamics and their quantum origin [6–35]. The following questions come to mind:

- How do the laws of thermodynamics emerge from quantum mechanics?
- What are the requirements of a theory to describe quantum mechanics and thermodynamics on a common ground?
- What are the fundamental reasons for tradeoff between power and efficiency?
- Do quantum devices operating far from equilibrium follow thermodynamical rules?
- Can quantum phenomena affect the performance of heat engines and refrigerators?

These issues are addressed by analyzing quantum models of heat engines and refrigerators. Extreme care has been taken to choose a model which can be analyzed from first principles. Two types of models are considered, continuous operating models resembling turbines and discrete four stroke reciprocating engines. The present review will focus on continuous devices.

II. THE CONTINUOUS ENGINE

An engine is a device that converts one form of energy to another: heat to work. In this conversion, part of heat from the hot bath is ejected to the cold bath limiting the efficiency of power generation. This is the essence of the second-law of thermodynamics.

A heat engine employs the natural current from a hot to a cold bath to generate power. The Carnot engine is a model of such a device. Carnot was able to incorporate the practical knowledge on steam engines of his era into a universal scientific statement on maximum efficiency [1]. Out of this insight the laws of thermodynamics were later formulated. This theme of *learning from an example* is typical in thermodynamics and will be employed to obtain insight from analysis of quantum devices.

A continuous engine operates in an autonomous fashion attaining steady state mode of operation. The analysis therefore requires an evaluation of steady state energy currents. The operating part of the device is connected simultaneously to the hot, cold and power output leads. The primary macroscopic example is a steam or gas turbine. The primary quantum heat engine is the laser. These devices share a universal aspect exemplified by the equivalence of the 3-level laser with the Carnot engine.

Reversing the operation of a heat engine generates a heat pump or a refrigerator. We will review the basic principles of quantum continuous engines and then invert their operation and study quantum refrigerators.

A. The quantum 3 level system as a heat engine

A contemporary example of a Carnot engine is the 3-level amplifier. The principle of operation is to convert population inversion into output power in the form of light. Heat gradients are employed to achieve this goal. Fig 1 shows its schematic construction. A hot reservoir characterised by temperature T_h induces transitions between the ground state ϵ_0 and the excited state ϵ_2 . When equilibrium is reached, the population ratio between these levels becomes

$$\frac{p_2}{p_0} = e^{-\frac{\hbar\omega_h}{k_B T_h}}$$

where $\omega_h \equiv \omega_{20} = (\epsilon_2 - \epsilon_0)/\hbar$ is the Bohr frequency and k_B is the Boltzmann constant. The cold reservoir at temperature T_c couples level ϵ_0 and level ϵ_1 meaning that:

$$\frac{p_1}{p_0} = e^{-\frac{\hbar\omega_c}{k_B T_c}},$$

where $\omega_c \equiv \omega_{10} = (\epsilon_1 - \epsilon_0)/\hbar$. The amplifier operates by coupling the energy levels ϵ_3 and ϵ_2 to the radiation field generating an output frequency which on resonance is $\nu = (\epsilon_3 - \epsilon_2)/\hbar$. The necessary condition for amplification is positive gain or population inversion defined by:

$$G = p_2 - p_1 \geq 0. \quad (1)$$

From this condition, by dividing by p_0 we obtain $e^{-\frac{\hbar\omega_h}{k_B T_h}} - e^{-\frac{\hbar\omega_c}{k_B T_c}} \geq 0$, which leads to:

$$\frac{\omega_c}{\omega_h} \equiv \frac{\omega_{10}}{\omega_{20}} \geq \frac{T_c}{T_h}, \quad (2)$$

The efficiency of the amplifier is defined by the ratio of the output energy $\hbar\nu$ to the energy extracted from the hot reservoir $\hbar\omega_{20}$:

$$\eta_o = \frac{\nu}{\omega_{20}} = 1 - \frac{\omega_c}{\omega_h}. \quad (3)$$

Eq. (3) is termed the quantum Otto efficiency [23]. Inserting the positive gain condition Eq. (1) and Eq. (2) the efficiency is limited by Carnot [1]:

$$\eta_o \leq \eta_c \equiv 1 - \frac{T_c}{T_h}. \quad (4)$$

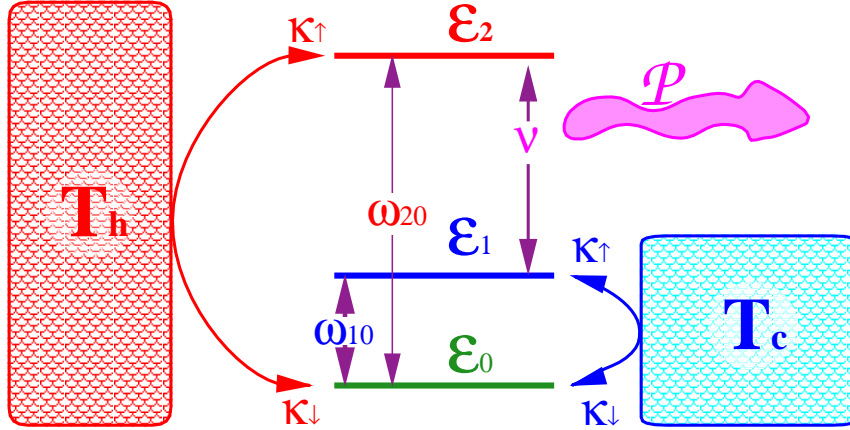


FIG. 1: The quantum 3-level amplifier as a Carnot heat engine. The system is coupled to a hot bath with temperature T_h and to a cold bath with temperature T_c . The output \mathcal{P} is a radiation field with frequency ν . (In the figure $\hbar = 1$). Power is generated provided there is population inversion between level ϵ_2 and ϵ_1 : $p_2 > p_1$. The hot bath equilibrates levels ϵ_0 and ϵ_2 via the rates $k \uparrow$ and $k \downarrow$ such that $k \uparrow / k \downarrow = \exp(\hbar\omega_{20}/k_B T_h)$. The efficiency $\eta = \nu/\omega_{20} \leq 1 - T_c/T_h$. Reversing the direction of operation using power to drive population from level ϵ_1 to ϵ_2 generates a heat pump then $p_2 < p_1$.

This result connecting the efficiency of a quantum amplifier to the Carnot efficiency was first obtained by Scuville et al. [6, 7].

The above description of the 3-level amplifier is based on a static quasi-equilibrium viewpoint. Real engines which produce power operate far from equilibrium conditions. Typically, their performance is restricted by friction, heat transport and heat leaks. A dynamical viewpoint is therefore the next required step.

B. The quantum tricycle

A quantum description enables to incorporate dynamics into thermodynamics. The tricycle model is the template for almost all continuous engines Cf. Fig. 2. This model will be employed to incorporate the quantum dynamics of the devices. Surprisingly very simple models exhibit the same features of engines generating finite power. Their efficiency at operating conditions is lower than the Carnot efficiency. In addition, heat leaks restrict the performance meaning that reversible operation is unattainable.

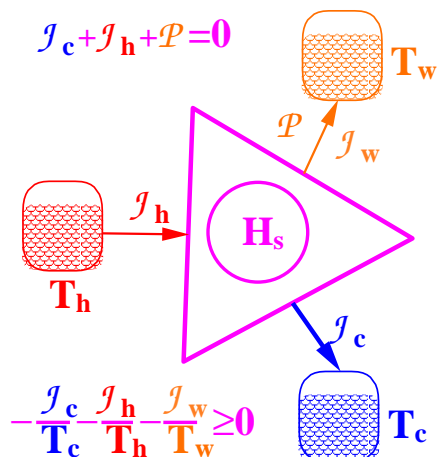


FIG. 2: The quantum tricycle: A quantum device coupled simultaneously to a hot, cold and power reservoir. Reversing the heat currents constructs a quantum refrigerator.

The tricycle engine has a generic structure displayed in Fig. 2.

- The basic model consists of three thermal baths: a hot bath with temperature T_h , a cold bath with temperature T_c and a work bath with temperature T_w .
- Each bath is connected to the engine via a frequency filter which we will model by three oscillators:

$$\hat{\mathbf{H}}_F = \hbar\omega_h \hat{\mathbf{a}}^\dagger \hat{\mathbf{a}} + \hbar\omega_c \hat{\mathbf{b}}^\dagger \hat{\mathbf{b}} + \hbar\omega_w \hat{\mathbf{c}}^\dagger \hat{\mathbf{c}} \quad , \quad (5)$$

where ω_h , ω_c and ω_w are the filter frequencies on resonance $\omega_w = \omega_h - \omega_c$.

- The device operates as an engine by removing an excitation from the hot bath and generating excitations on the cold and work reservoirs. In second quantization formalism the Hamiltonian describing such an interaction becomes:

$$\hat{\mathbf{H}}_I = \hbar\epsilon \left(\hat{\mathbf{a}} \hat{\mathbf{b}}^\dagger \hat{\mathbf{c}}^\dagger + \hat{\mathbf{a}}^\dagger \hat{\mathbf{b}} \hat{\mathbf{c}} \right) \quad , \quad (6)$$

where ϵ is the coupling strength.

- The device operates as a refrigerator by removing an excitation from the cold bath as well as from the work bath and generating an excitation in the hot bath. The term $\hat{\mathbf{a}}^\dagger \hat{\mathbf{b}} \hat{\mathbf{c}}$ in the Hamiltonian of Eq. (6) describes this action. (Cf. Section III).

Some comments are appropriate:

1. Different types of heat baths can be employed which can include bosonic baths composed of phonons or photons, or fermionic baths composed of electrons. The frequency filters select from the continuous spectrum of the bath the working component to be employed in the tricycle. These frequency filters can be constructed also from two-level-systems (TLS) or formulated as qubits [36–38].
2. The interaction term Eq. (6), is strictly non-linear, incorporating three heat currents simultaneously. This crucial fact has important consequences. A linear device cannot operate as a heat engine or refrigerator [39]. A linear device is constructed from a network of harmonic oscillators with linear connections of the type $\hbar\mu_{ij} (\hat{\mathbf{a}}_i\hat{\mathbf{a}}_j^\dagger + \hat{\mathbf{a}}_i^\dagger\hat{\mathbf{a}}_j)$ with some connections to harmonic heat baths. In such a device the hottest bath always cools down and the coldest bath always heats up. Thus, this construction can transport heat but not generate power since power is equivalent to transporting heat to an infinitely hot reservoir. Another flaw in a linear model is that the different bath modes do not equilibrate with each other. A generic bath should equilibrate any system Hamiltonian irrespective of its frequency.
3. Many nonlinear interaction Hamiltonians of the type $\hat{\mathbf{H}}_I = \hat{\mathbf{A}} \otimes \hat{\mathbf{B}} \otimes \hat{\mathbf{C}}$ can lead to a working heat engine. These Hamiltonians can be reduced to the form of Eq. (6) which captures the essence of such interactions.

The first-law of thermodynamics represents the energy balance of heat currents originating from the three baths and collimating on the system:

$$\frac{dE_s}{dt} = \mathcal{J}_h + \mathcal{J}_c + \mathcal{J}_w \quad . \quad (7)$$

At steady state no heat is accumulated in the tricycle, thus $\frac{dE_s}{dt} = 0$. In addition, in steady state the entropy is only generated in the baths, leading to the second-law of thermodynamics:

$$\frac{d}{dt}\Delta\mathcal{S}_u = -\frac{\mathcal{J}_h}{T_h} - \frac{\mathcal{J}_c}{T_c} - \frac{\mathcal{J}_w}{T_w} \geq 0 \quad . \quad (8)$$

This version of the second-law is a generalisation of the statement of Clausius; heat does not flow spontaneously from cold to hot bodies [40]. When the temperature $T_w \rightarrow \infty$, no entropy is generated in the power bath. An energy current with no accompanying entropy production is equivalent to generating pure power: $\mathcal{P} = \mathcal{J}_w$, where \mathcal{P} is the output power.

The evaluation of the currents \mathcal{J}_j in the tricycle model requires dynamical equations of motion. The major assumption is that the total systems is closed and its dynamics is generated by the global Hamiltonians.

$$\hat{\mathbf{H}} = \hat{\mathbf{H}}_0 + \hat{\mathbf{H}}_{SB} . \quad (9)$$

This Hamiltonian $\hat{\mathbf{H}}_0$ includes the bare system and the heat baths:

$$\hat{\mathbf{H}}_0 = \hat{\mathbf{H}}_s + \hat{\mathbf{H}}_H + \hat{\mathbf{H}}_C + \hat{\mathbf{H}}_W , \quad (10)$$

where the system Hamiltonian $\hat{\mathbf{H}}_s = \hat{\mathbf{H}}_I + \hat{\mathbf{H}}_h + \hat{\mathbf{H}}_c + \hat{\mathbf{H}}_w$ consists of three energy filtering components and an interaction part with an external field. The reservoir Hamiltonians are the hot $\hat{\mathbf{H}}_H$, cold $\hat{\mathbf{H}}_C$ and work $\hat{\mathbf{H}}_W$. The system-bath interaction Hamiltonian: $\hat{\mathbf{H}}_{SB} = \hat{\mathbf{H}}_{sH} + \hat{\mathbf{H}}_{sC} + \hat{\mathbf{H}}_{sW}$.

A thermodynamical idealisation assumes that the tricycle system and the baths are uncorrelated, meaning that the total state of the combined system becomes a tensor product at all times [32]:

$$\hat{\rho} = \hat{\rho}_s \otimes \hat{\rho}_H \otimes \hat{\rho}_C \otimes \hat{\rho}_W . \quad (11)$$

Under these conditions the dynamical equations of motion for the tricycle become:

$$\frac{d}{dt}\hat{\rho}_s = \mathcal{L}\hat{\rho}_s , \quad (12)$$

where \mathcal{L} is the Liouville superoperator described in terms of the system Hilbert space, where the reservoirs are described implicitly. Within the formalism of quantum open system, \mathcal{L} can take the form of the Gorini-Kossakowski-Sudarshan-Lindblad (GKS-L) Markovian generator [41, 42].

Thermodynamics is notorious in employing a very small number of variables. In equilibrium conditions the knowledge of the Hamiltonian is sufficient. When deviating from equilibrium additional observables are added. This suggest presenting the dynamical generator in Heisenberg form for arbitrary system operators $\hat{\mathbf{O}}_s$:

$$\frac{d}{dt}\hat{\mathbf{O}}_s = \mathcal{L}^*\hat{\mathbf{O}}_s = \frac{i}{\hbar}[\hat{\mathbf{H}}_s, \hat{\mathbf{O}}_s] + \sum_k \hat{\mathbf{V}}_k \hat{\mathbf{O}}_s \hat{\mathbf{V}}_k^\dagger - \frac{1}{2}\{\hat{\mathbf{V}}_k \hat{\mathbf{V}}_k^\dagger, \hat{\mathbf{O}}_s\} . \quad (13)$$

The operators $\hat{\mathbf{V}}_k$ are system operators still to be determined. The task of evaluating the modified system Hamiltonian $\hat{\mathbf{H}}_s$ and the operators $\hat{\mathbf{V}}_k$ is made extremely difficult due to the nonlinear interaction in Eq. (6). Any progress from this point requires a specific description of the heat baths and approximations to deal with the nonlinear terms.

C. The quantum amplifier

The quantum amplifier is the most elementary quantum continuous heat engine converting heat to work. The purpose is to generate power from a temperature difference between the hot and cold reservoirs. The output power is described by a time dependent external field.

The general device Hamiltonian is therefore time dependent:

$$\hat{\mathbf{H}}_s(t) = \hat{\mathbf{H}}_0 + \hat{\mathbf{V}}(t) . \quad (14)$$

The Markovian master equation in Heisenberg form for the system operator $\hat{\mathbf{O}}_s$ when the system coupled to the hot and cold bath:

$$\frac{d}{dt} \hat{\mathbf{O}}_s = \frac{i}{\hbar} [\hat{\mathbf{H}}(t), \hat{\mathbf{O}}_s(t)] + \mathcal{L}_h^*(\hat{\mathbf{O}}_s(t)) + \mathcal{L}_c^*(\hat{\mathbf{O}}_s(t)) . \quad (15)$$

The change in energy of the device is obtained by replacing $\hat{\mathbf{O}}_s$ by $\hat{\mathbf{H}}_s$:

$$\frac{dE_s}{dt} = \langle \mathcal{L}_h^*(\hat{\mathbf{H}}_s) \rangle + \langle \mathcal{L}_c^*(\hat{\mathbf{H}}_s) \rangle + \langle \frac{\partial \hat{\mathbf{H}}_s}{\partial t} \rangle . \quad (16)$$

Equation (16) can be interpreted as the time derivative of the first law of thermodynamics [8, 32, 43, 44] based on the Markovian GKS-L generator. Power is identified as:

$$\mathcal{P} = \langle \frac{\partial H_s}{\partial t} \rangle , \quad (17)$$

and the heat current as:

$$\mathcal{J}_h = \langle \mathcal{L}_h^*(\hat{\mathbf{H}}_s) \rangle , \quad \mathcal{J}_c = \langle \mathcal{L}_c^*(\hat{\mathbf{H}}_s) \rangle . \quad (18)$$

The partition between the Hamiltonian and the dissipative part in the GKS-L generator is not unique [32]. A unique derivation of the Master equation based on the weak coupling limit leads to dynamics which is consistent with the first and second laws of thermodynamics [45].

The template of the tricycle model is employed to describe the dynamics of the amplifier. The interaction Hamiltonian is modified to become:

$$\hat{\mathbf{H}}_I(t) = \hbar\epsilon \left(\hat{\mathbf{a}} \hat{\mathbf{b}}^\dagger e^{+i\nu t} + \hat{\mathbf{a}}^\dagger \hat{\mathbf{b}} e^{-i\nu t} \right) , \quad (19)$$

where $\nu \equiv \omega_w$ is the frequency of the time dependent driving field and ϵ is the coupling amplitude. The modification of Eq. (6) eliminates the nonlinearity, it amounts to replacing the operator $\hat{\mathbf{c}}$ and $\hat{\mathbf{c}}^\dagger$ by a c-number. The amplifier output power becomes:

$$\mathcal{P} = \hbar\epsilon\nu \left(\langle \hat{\mathbf{a}}\hat{\mathbf{b}}^\dagger \rangle e^{+i\nu t} - \langle \hat{\mathbf{a}}^\dagger\hat{\mathbf{b}} \rangle e^{-i\nu t} \right). \quad (20)$$

After the nonlinearity has been eliminated the quantum Master equation for the amplifier can be derived from first principles based on the weak system bath coupling expansion. This approximation is a thermodynamic idealisation equivalent to an isothermal partition between the system and baths [32].

The interaction with the baths is given by

$$\hat{\mathbf{H}}_{sb} = \lambda_a(\hat{\mathbf{a}} + \hat{\mathbf{a}}^\dagger) \otimes \hat{\mathbf{R}}_h + \lambda_b(\hat{\mathbf{b}} + \hat{\mathbf{b}}^\dagger) \otimes \hat{\mathbf{R}}_c. \quad (21)$$

where $\hat{\mathbf{R}}$ are reservoir operators and λ is the small system-bath coupling parameter. A crucial step has to be performed before this procedure is applied. The system Hamiltonian has to be rediagonalized with the interaction before the system is coupled to the baths. This diagonalization modifies the frequencies of the system resulting in a splitting of the filter frequencies. The prediagonalization is crucial for the master equations to be consistent with the second-law of thermodynamics [9, 38, 46].

The main ingredients of the derivation:

I) Transformation to interaction picture. The reservoir coupling operators $\hat{\mathbf{R}}$ transform according to the free baths Hamiltonian, and the system operators are subject to the unitary propagator which under resonance conditions becomes:

$$\hat{\mathbf{U}}_s(t, 0) = \mathcal{T} \exp \left\{ -\frac{i}{\hbar} \int_0^t \hat{\mathbf{H}}(s) ds \right\} = e^{-\frac{i}{\hbar} \hat{\mathbf{H}}_0 t} e^{-\frac{i}{\hbar} \hat{\mathbf{V}} t}, \quad (22)$$

where

$$\hat{\mathbf{H}}_0 = \hbar\omega_h \hat{\mathbf{a}}^\dagger \hat{\mathbf{a}} + \hbar\omega_c \hat{\mathbf{b}}^\dagger \hat{\mathbf{b}}, \quad \hat{\mathbf{V}} = \hbar\epsilon(\hat{\mathbf{a}}^\dagger \hat{\mathbf{b}} + \hat{\mathbf{a}} \hat{\mathbf{b}}^\dagger). \quad (23)$$

II) Fourier decomposition of the interaction part. The operators in the interaction picture take the form

$$\begin{aligned} \tilde{\mathbf{a}}(\mathbf{t}) &= \hat{\mathbf{U}}_s(\mathbf{t}, \mathbf{0})^\dagger \hat{\mathbf{a}} \hat{\mathbf{U}}_s(\mathbf{t}, \mathbf{0}) = \\ &e^{\frac{i}{\hbar} \hat{\mathbf{V}} t} \left[e^{\frac{i}{\hbar} \hat{\mathbf{H}}_0 t} \hat{\mathbf{a}} e^{-\frac{i}{\hbar} \hat{\mathbf{H}}_0 t} \right] e^{-\frac{i}{\hbar} \hat{\mathbf{V}} t} = \cos(\epsilon t) e^{-i\omega_h t} \hat{\mathbf{a}} - i \sin(\epsilon t) e^{-i\omega_h t} \hat{\mathbf{b}}, \end{aligned} \quad (24)$$

and a similar equation for $\tilde{\mathbf{b}}(t)$. The Fourier decomposition becomes:

$$\tilde{\mathbf{a}}(\mathbf{t}) = \frac{1}{\sqrt{2}}(\mathbf{e}^{-i(\omega_h^+)t}\tilde{\mathbf{d}}_+ + \mathbf{e}^{-i(\omega_h^-)t}\tilde{\mathbf{d}}_-) \quad (25)$$

and

$$\tilde{\mathbf{b}}(\mathbf{t}) = \frac{1}{\sqrt{2}}(\mathbf{e}^{-i(\omega_c^+)t}\tilde{\mathbf{d}}_+ - \mathbf{e}^{-i(\omega_c^-)t}\tilde{\mathbf{d}}_-) \quad (26)$$

where $\tilde{\mathbf{d}}_+ = \frac{\tilde{\mathbf{a}}+\tilde{\mathbf{b}}}{\sqrt{2}}$, $\tilde{\mathbf{d}}_- = \frac{\tilde{\mathbf{a}}-\tilde{\mathbf{b}}}{\sqrt{2}}$ and $\omega_{h(c)}^\pm = (\omega_{h(c)} \pm \epsilon)$. Similarly $\tilde{\mathbf{a}}^\dagger(\mathbf{t})$, $\tilde{\mathbf{b}}^\dagger(\mathbf{t})$ are evaluated.

III) Performing the system-bath weak coupling approximation. This approximation involves averaging over fast oscillating terms with typical frequencies $\sim 2\omega_c, 2\omega_h, 2\epsilon$. This approximation is restricted to conditions that the relaxation time of the open system is much longer than the intrinsic time scale $\omega_c^{-1}, \omega_h^{-1}$ and ϵ^{-1} . Thus, terms oscillating rapidly over the relaxation time average out. Such equations were derived in Ref.[36]. If the coupling to the external field is weak, such that $\omega_h, \omega_c \gg \epsilon$ and the relaxation time of the open system is comparable with ϵ^{-1} , the derivation is modified accordingly. In this case there is no justification to neglect terms oscillating with frequency $\sim \epsilon$. Keeping such terms, the total time-dependent (interaction picture) generator has the form:

$$\mathcal{L}(t) = \mathcal{L}_h^{(+)} + \mathcal{L}_h^{(-)} + \mathcal{L}_c^{(+)} + \mathcal{L}_c^{(-)}, \quad (27)$$

where

$$\begin{aligned} \mathcal{L}_h^{(+)} \hat{\rho} &= \frac{1}{4}\gamma_h^{(+)}([\tilde{\mathbf{d}}_+, \hat{\rho}\tilde{\mathbf{d}}_+] + [\tilde{\mathbf{d}}_-, \hat{\rho}\tilde{\mathbf{d}}_+]e^{i2\epsilon t} + e^{-\beta\hbar\omega_h^+}([\tilde{\mathbf{d}}_+^\dagger, \hat{\rho}\tilde{\mathbf{d}}_+] + [\tilde{\mathbf{d}}_-^\dagger, \hat{\rho}\tilde{\mathbf{d}}_+]e^{-i2\epsilon t}) + h.c) \\ \mathcal{L}_c^{(+)} \hat{\rho} &= \frac{1}{4}\gamma_c^{(+)}([\tilde{\mathbf{d}}_+, \hat{\rho}\tilde{\mathbf{d}}_+] - [\tilde{\mathbf{d}}_-, \hat{\rho}\tilde{\mathbf{d}}_+]e^{i2\epsilon t} + e^{-\beta\hbar\omega_c^+}([\tilde{\mathbf{d}}_+^\dagger, \hat{\rho}\tilde{\mathbf{d}}_+] - [\tilde{\mathbf{d}}_-^\dagger, \hat{\rho}\tilde{\mathbf{d}}_+]e^{-i2\epsilon t}) + h.c) \\ \mathcal{L}_h^{(-)} \hat{\rho} &= \frac{1}{4}\gamma_h^{(-)}([\tilde{\mathbf{d}}_-, \hat{\rho}\tilde{\mathbf{d}}_-] + [\tilde{\mathbf{d}}_+, \hat{\rho}\tilde{\mathbf{d}}_-]e^{-i2\epsilon t} + e^{-\beta\hbar\omega_h^-}([\tilde{\mathbf{d}}_-^\dagger, \hat{\rho}\tilde{\mathbf{d}}_-] + [\tilde{\mathbf{d}}_+^\dagger, \hat{\rho}\tilde{\mathbf{d}}_-]e^{i2\epsilon t}) + h.c) \\ \mathcal{L}_c^{(-)} \hat{\rho} &= \frac{1}{4}\gamma_c^{(-)}([\tilde{\mathbf{d}}_-, \hat{\rho}\tilde{\mathbf{d}}_-] - [\tilde{\mathbf{d}}_+, \hat{\rho}\tilde{\mathbf{d}}_-]e^{-i2\epsilon t} + e^{-\beta\hbar\omega_c^-}([\tilde{\mathbf{d}}_-^\dagger, \hat{\rho}\tilde{\mathbf{d}}_-] - [\tilde{\mathbf{d}}_+^\dagger, \hat{\rho}\tilde{\mathbf{d}}_-]e^{i2\epsilon t}) + h.c) \end{aligned} \quad (28)$$

and the inverse temperature is $\beta = \hbar/k_B T$. The relaxation rates $\gamma_{h(c)}^{(\pm)} = \gamma_{h(c)}(\omega_{h(c)} \pm \epsilon)$, have the structure:

$$\gamma(\omega) = \lambda^2 \int_{-\infty}^{\infty} e^{i\omega t} Tr(\hat{\rho}_R e^{\frac{i}{\hbar}\hat{\mathbf{H}}_R t} \hat{\mathbf{R}} e^{-\frac{i}{\hbar}\hat{\mathbf{H}}_R t} \hat{\mathbf{R}}) dt \quad (29)$$

and can be calculated explicitly for different types of heat baths.

Note that if we neglect the time dependent terms in Eq. (28) the master equation derived in Ref. [36] is recovered. The generators in Eq.(28) are not in GKS-L completely positive

semigroup form. To correct this flaw, off-diagonal terms are added to the master equation recovering the first standard form, i.e. $\mathcal{L}_D \hat{\rho} = \sum_{i,j} C_{i,j} \left(\hat{\mathbf{F}}_i \hat{\rho} \hat{\mathbf{F}}_j^\dagger - \frac{1}{2} \{ \hat{\mathbf{F}}_j^\dagger \hat{\mathbf{F}}_i, \hat{\rho} \} \right)$. Next, we insure that these terms will not contribute twice by rescaling the kinetic coefficients. In order to verify that the map is completely positive, it is sufficient that the matrix $(C_{i,j})$ is positive definite. The modified GKS-L master equations now become:

$$\begin{aligned} \mathcal{L}_h^{(\pm)} \hat{\rho} &= \frac{1}{2} \gamma_h^{(\pm)} \left(\tilde{\mathbf{d}}_\pm \hat{\rho} \tilde{\mathbf{d}}_\pm^\dagger - \frac{1}{2} \{ \tilde{\mathbf{d}}_\pm^\dagger \tilde{\mathbf{d}}_\pm, \hat{\rho} \} + e^{-\beta_h \omega_h^\pm} \left(\tilde{\mathbf{d}}_\pm^\dagger \hat{\rho} \tilde{\mathbf{d}}_\pm - \frac{1}{2} \{ \tilde{\mathbf{d}}_\pm \tilde{\mathbf{d}}_\pm^\dagger, \hat{\rho} \} \right) \right) \\ &+ \frac{1}{4} \gamma_h^{(\pm)} \left(\tilde{\mathbf{d}}_- \hat{\rho} \tilde{\mathbf{d}}_+^\dagger - \frac{1}{2} \{ \tilde{\mathbf{d}}_+^\dagger \tilde{\mathbf{d}}_-, \hat{\rho} \} + e^{-\beta_h \omega_h^\pm} \left(\tilde{\mathbf{d}}_+^\dagger \hat{\rho} \tilde{\mathbf{d}}_- - \frac{1}{2} \{ \tilde{\mathbf{d}}_- \tilde{\mathbf{d}}_+^\dagger, \hat{\rho} \} \right) \right) e^{i2\epsilon t} \\ &+ \frac{1}{4} \gamma_h^{(\pm)} \left(\tilde{\mathbf{d}}_+ \hat{\rho} \tilde{\mathbf{d}}_-^\dagger - \frac{1}{2} \{ \tilde{\mathbf{d}}_-^\dagger \tilde{\mathbf{d}}_+, \hat{\rho} \} + e^{-\beta_h \omega_h^\pm} \left(\tilde{\mathbf{d}}_-^\dagger \hat{\rho} \tilde{\mathbf{d}}_+ - \frac{1}{2} \{ \tilde{\mathbf{d}}_+ \tilde{\mathbf{d}}_-^\dagger, \hat{\rho} \} \right) \right) e^{-i2\epsilon t} \end{aligned} \quad (30)$$

$$\begin{aligned} \mathcal{L}_c^{(\pm)} \hat{\rho} &= \frac{1}{2} \gamma_c^{(\pm)} \left(\tilde{\mathbf{d}}_\pm \hat{\rho} \tilde{\mathbf{d}}_\pm^\dagger - \frac{1}{2} \{ \tilde{\mathbf{d}}_\pm^\dagger \tilde{\mathbf{d}}_\pm, \hat{\rho} \} + e^{-\beta_c \omega_c^\pm} \left(\tilde{\mathbf{d}}_\pm^\dagger \hat{\rho} \tilde{\mathbf{d}}_\pm - \frac{1}{2} \{ \tilde{\mathbf{d}}_\pm \tilde{\mathbf{d}}_\pm^\dagger, \hat{\rho} \} \right) \right) \\ &- \frac{1}{4} \gamma_c^{(\pm)} \left(\tilde{\mathbf{d}}_- \hat{\rho} \tilde{\mathbf{d}}_+^\dagger - \frac{1}{2} \{ \tilde{\mathbf{d}}_+^\dagger \tilde{\mathbf{d}}_-, \hat{\rho} \} + e^{-\beta_c \omega_c^\pm} \left(\tilde{\mathbf{d}}_+^\dagger \hat{\rho} \tilde{\mathbf{d}}_- - \frac{1}{2} \{ \tilde{\mathbf{d}}_- \tilde{\mathbf{d}}_+^\dagger, \hat{\rho} \} \right) \right) e^{i2\epsilon t} \\ &- \frac{1}{4} \gamma_c^{(\pm)} \left(\tilde{\mathbf{d}}_+ \hat{\rho} \tilde{\mathbf{d}}_-^\dagger - \frac{1}{2} \{ \tilde{\mathbf{d}}_-^\dagger \tilde{\mathbf{d}}_+, \hat{\rho} \} + e^{-\beta_c \omega_c^\pm} \left(\tilde{\mathbf{d}}_-^\dagger \hat{\rho} \tilde{\mathbf{d}}_+ - \frac{1}{2} \{ \tilde{\mathbf{d}}_+ \tilde{\mathbf{d}}_-^\dagger, \hat{\rho} \} \right) \right) e^{-i2\epsilon t} \end{aligned}$$

Note that the rotating term $e^{-i2\epsilon t}$ can be absorbed in $\tilde{\mathbf{d}}$ by a second rotation of the frame. The derivation of the Master equation, Eq. (30), for a driven system is a delicate task. The pre-diagonalization step ensures consistency with the second-law [9, 46, 47].

1. Solving the equations of motion for the engine

In thermodynamic tradition, the engine is well described by a small set of observables. They in turn are represented by operators defining the heat currents in the engine. To exploit this property the Hamiltonian is transformed to the interaction frame:

$$\hat{\mathbf{H}}_I(t) = \hat{\mathbf{U}}_s^\dagger(t, 0) \hat{\mathbf{H}}(t) \hat{\mathbf{U}}_s(t, 0) = \hbar \frac{\omega_h + \omega_c}{2} \hat{\mathbf{W}} + \hbar \frac{\omega_h - \omega_c}{2} \hat{\mathbf{X}} + \hbar \epsilon \hat{\mathbf{Z}} \quad (31)$$

where the operators are closed to commutation relations, forming the SU(2) Lie algebra:

$$\begin{aligned} \hat{\mathbf{W}} &= (\tilde{\mathbf{d}}_+^\dagger \tilde{\mathbf{d}}_+ + \tilde{\mathbf{d}}_-^\dagger \tilde{\mathbf{d}}_-) \quad , \quad \hat{\mathbf{X}} = (\tilde{\mathbf{d}}_+^\dagger \tilde{\mathbf{d}}_- e^{i2\epsilon t} + \tilde{\mathbf{d}}_-^\dagger \tilde{\mathbf{d}}_+ e^{-i2\epsilon t}), \\ \hat{\mathbf{Y}} &= i(\tilde{\mathbf{d}}_+^\dagger \tilde{\mathbf{d}}_- e^{i2\epsilon t} - \tilde{\mathbf{d}}_-^\dagger \tilde{\mathbf{d}}_+ e^{-i2\epsilon t}) \quad , \quad \hat{\mathbf{Z}} = (\tilde{\mathbf{d}}_+^\dagger \tilde{\mathbf{d}}_+ - \tilde{\mathbf{d}}_-^\dagger \tilde{\mathbf{d}}_-). \end{aligned}$$

The dynamical description of the engine is completely determined by the expectation values

of the operators constituting the SU(2) algebra. The equation of motion for these operators which are closed to this set follow Eq. (30) in Heisenberg form:

$$\begin{aligned}\frac{d\hat{\mathbf{W}}}{dt} &= -\frac{1}{4}\Gamma_T\hat{\mathbf{W}} - \frac{1}{4}(\Gamma^+ - \Gamma^-)\hat{\mathbf{Z}} - \frac{1}{4}(\Gamma_h - \Gamma_c)\hat{\mathbf{X}} + \frac{1}{2}(\Gamma_h^+N_h^+ + \Gamma_h^-N_h^- + \Gamma_c^+N_c^+ + \Gamma_c^-N_c^-) \\ \frac{d\hat{\mathbf{X}}}{dt} &= -\frac{1}{4}\Gamma_T\hat{\mathbf{X}} - \frac{1}{4}(\Gamma_h - \Gamma_c)\hat{\mathbf{W}} + \frac{1}{2}(\Gamma_h^+N_h^+ + \Gamma_h^-N_h^- - \Gamma_c^+N_c^+ - \Gamma_c^-N_c^-) + 2\epsilon\hat{\mathbf{Y}} \\ \frac{d\hat{\mathbf{Y}}}{dt} &= -\frac{1}{4}\Gamma_T\hat{\mathbf{Y}} - 2\epsilon\hat{\mathbf{X}}\end{aligned}\tag{32}$$

$$\frac{d\hat{\mathbf{Z}}}{dt} = -\frac{1}{4}\Gamma_T\hat{\mathbf{Z}} - \frac{1}{4}(\Gamma^+ - \Gamma^-)\hat{\mathbf{W}} + \frac{1}{2}(\Gamma_h^+N_h^+ - \Gamma_h^-N_h^- + \Gamma_c^+N_c^+ - \Gamma_c^-N_c^-),$$

where the equilibrium populations of the dressed filter operators and heat transport coefficients become:

$$N_{h(c)}^\pm = \frac{1}{\exp\left(\frac{\hbar\omega_{h(c)}^\pm}{k_B T_{h(c)}}\right) - 1}, \quad \Gamma_{h(c)}^\pm = \gamma_{h(c)}^\pm (1 - \exp\left(-\frac{\hbar\omega_{h(c)}^\pm}{k_B T_{h(c)}}\right))\tag{33}$$

with $\omega_{h(c)}^\pm = \omega_{h(c)} \pm \epsilon$ and

$$\Gamma_T = \Gamma_h^+ + \Gamma_h^- + \Gamma_c^+ + \Gamma_c^-, \quad \Gamma^\pm = \Gamma_h^\pm + \Gamma_c^\pm, \quad \Gamma_{h(c)} = \Gamma_{h(c)}^+ + \Gamma_{h(c)}^-. \tag{34}$$

A simplifying limit is obtained when the relaxation rate of the upper and lower manifold are approximately equal: $\Gamma_h^+ = \Gamma_h^- \equiv \kappa_h$ and $\Gamma_c^+ = \Gamma_c^- \equiv \kappa_c$. For a typical harmonic bath where $\Gamma(\omega) \sim \omega^d$, and d stands for the bath dimension, this is a good approximation ($\omega_h, \omega_c \gg \epsilon$).

The equations of motion for the amplifier relax to a steady state operational mode. The expectation values for the operators in steady state $\frac{d\hat{\mathbf{X}}}{dt} = \frac{d\hat{\mathbf{Y}}}{dt} = \frac{d\hat{\mathbf{Z}}}{dt} = \frac{d\hat{\mathbf{W}}}{dt} = 0$ become:

$$\begin{aligned}\langle \hat{\mathbf{X}} \rangle &= \frac{\kappa_h \kappa_c (N_h^+ + N_h^- - N_c^+ - N_c^-)}{2(4\epsilon^2 + \kappa_h \kappa_c)} \\ \langle \hat{\mathbf{Y}} \rangle &= -\frac{2\epsilon(N_h^+ + N_h^- - N_c^+ - N_c^-)}{4\epsilon^2 + \kappa_h \kappa_c} \left(\frac{\kappa_h \kappa_c}{\kappa_h + \kappa_c} \right) \\ \langle \hat{\mathbf{Z}} \rangle &= \frac{(N_h^+ - N_h^-)\kappa_h + (N_c^+ - N_c^-)\kappa_c}{\kappa_h + \kappa_c} \\ \langle \hat{\mathbf{W}} \rangle &= \frac{(N_h^+ + N_h^- + N_c^+ + N_c^-)\kappa_h \kappa_c}{2(4\epsilon^2 + \kappa_h \kappa_c)} + \frac{4\lambda^2((N_h^+ + N_h^-)\kappa_h + (N_c^+ + N_c^-)\kappa_c)}{(4\epsilon^2 + \kappa_h \kappa_c)(\kappa_h + \kappa_c)}.\end{aligned}\tag{35}$$

The commutator $[\hat{\mathbf{Y}}, \hat{\mathbf{H}}_I] \neq 0$ therefore $\hat{\mathbf{Y}}$ is related to the non diagonal elements of the Hamiltonian which define the coherence between energy levels.

The solution of the equation of motion lead to the thermodynamical observables at steady state conditions, the power and heat flows become:

$$\begin{aligned}\mathcal{P} &= \hbar\epsilon\nu \langle \hat{\mathbf{Y}} \rangle = -\frac{2\hbar(\omega_h - \omega_c)\epsilon^2 G_1}{4\epsilon^2 + \kappa_h \kappa_c} \left(\frac{\kappa_h \kappa_c}{\kappa_h + \kappa_c} \right) \\ \mathcal{J}_h &= \mathcal{L}_h^\dagger(\hat{\mathbf{H}}_I) = \left(\frac{\hbar\epsilon G_2}{2} + \frac{2\hbar\omega_h\epsilon^2 G_1}{4\epsilon^2 + \kappa_h \kappa_c} \right) \left(\frac{\kappa_h \kappa_c}{\kappa_h + \kappa_c} \right) \\ \mathcal{J}_c &= \mathcal{L}_c^\dagger(\hat{\mathbf{H}}_I) = -\left(\frac{\hbar\epsilon G_2}{2} + \frac{2\hbar\omega_c\epsilon^2 G_1}{4\epsilon^2 + \kappa_h \kappa_c} \right) \left(\frac{\kappa_h \kappa_c}{\kappa_h + \kappa_c} \right)\end{aligned}\quad (36)$$

where the generalised gain becomes:

$$\begin{aligned}G_1 &= (N_h^+ + N_h^-) - (N_c^+ + N_c^-) \\ G_2 &= (N_h^+ - N_h^-) - (N_c^+ - N_c^-)\end{aligned}\quad (37)$$

The first law of thermodynamics is satisfied such that $\mathcal{J}_h + \mathcal{J}_c + \mathcal{P} = 0$ as well as the second law: $-\frac{\mathcal{J}_h}{T_h} - \frac{\mathcal{J}_c}{T_c} \geq 0$. The power \mathcal{P} is proportional to the expectation value of the coherence $\langle \hat{\mathbf{Y}} \rangle$. As a consequence additional pure dephasing originating from external noise will degrade the power. Such noise generated by a Gaussian random process is described by the generator $\mathcal{L}_D = -\gamma^2[\hat{\mathbf{H}}_I, [\hat{\mathbf{H}}_I, \bullet]]$ [48].

In the regime where the external driving amplitude is larger than the heat conductivity $\epsilon^2 \gg \kappa_h \kappa_c$, Eq.(36) converges to the results of Ref. [36].

$$\begin{aligned}\mathcal{P} &= \hbar\epsilon\nu \langle \hat{\mathbf{Y}} \rangle = -\frac{1}{2}\hbar\nu G_1 \left(\frac{\kappa_h \kappa_c}{\kappa_h + \kappa_c} \right) \\ \mathcal{J}_h &= \mathcal{L}_h^\dagger(\hat{\mathbf{H}}_I) = \frac{1}{2}\hbar (\epsilon G_2 + \omega_h G_1) \left(\frac{\kappa_h \kappa_c}{\kappa_h + \kappa_c} \right) \\ \mathcal{J}_c &= \mathcal{L}_c^\dagger(\hat{\mathbf{H}}_I) = -\frac{1}{2}\hbar (\epsilon G_2 + \omega_c G_1) \left(\frac{\kappa_h \kappa_c}{\kappa_h + \kappa_c} \right)\end{aligned}\quad (38)$$

Returning to Eq. (36), optimal power is obtained when the heat conductances from the hot and cold bath are balanced: $\Gamma \equiv \kappa_c = \kappa_h$, then the power and the heat flows from the reservoirs become:

$$\begin{aligned}\mathcal{P} &= \hbar\epsilon\nu \langle \hat{\mathbf{Y}} \rangle = -\frac{\hbar\nu\epsilon^2\Gamma G_1}{4\epsilon^2 + \Gamma^2} \\ \mathcal{J}_h &= \mathcal{L}_h^\dagger(\hat{\mathbf{H}}_I) = \frac{\hbar\epsilon\Gamma G_2}{4} + \frac{\hbar\omega_h\epsilon^2\Gamma G_1}{4\epsilon^2 + \Gamma^2} \\ \mathcal{J}_c &= \mathcal{L}_c^\dagger(\hat{\mathbf{H}}_I) = -\frac{\hbar\epsilon\Gamma G_2}{4} - \frac{\hbar\omega_c\epsilon^2\Gamma G_1}{4\epsilon^2 + \Gamma^2}\end{aligned}\quad (39)$$

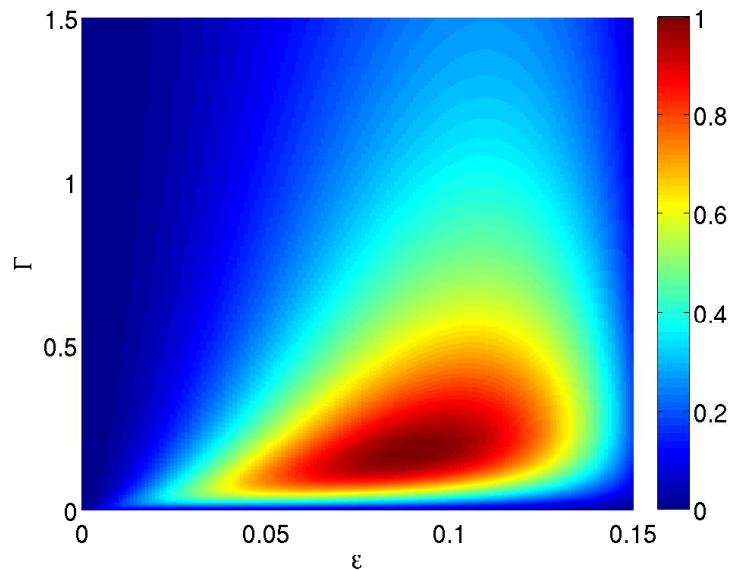


FIG. 3: The normalized power $\mathcal{P}/\mathcal{P}_{max}$ as a function of the coupling amplitude to the external field ϵ and the heat conductivity Γ . A clear maximum is obtained for $\Gamma = 2\epsilon$.

Figure 3 shows the power as a function of the heat conductivity coefficient Γ and the coupling to the external field ϵ . A clear global maximum is obtained for $\Gamma = 2\epsilon$.

The efficiency of the amplifier, is defined as $\eta = -\frac{\mathcal{P}}{\mathcal{J}_h}$. For the present model it becomes:

$$\eta = \frac{\nu}{\omega_h + \frac{(\Gamma^2 + \epsilon^2)G_2}{4|\epsilon|G_1}}. \quad (40)$$

In the limit of $\epsilon \rightarrow 0$ and $\Gamma \rightarrow 0$ the efficiency approaches the Otto value: $\eta_o = 1 - \frac{\omega_c}{\omega_h}$ and for zero gain, $\frac{\omega_c}{\omega_h} = \frac{T_c}{T_h}$, we obtain the Carnot limit $\eta_c = 1 - \frac{T_c}{T_h}$.

For finite fixed Γ the efficiency in the limit $\epsilon \rightarrow 0$ becomes:

$$\eta = \frac{\nu}{\omega_h + \frac{\Gamma^2 \left(T_h \left(1 - \cosh\left(\frac{\omega_h}{T_h}\right) \right) - T_c \left(1 - \cosh\left(\frac{\omega_c}{T_c}\right) \right) \right)}{4T_h T_c \left(\sinh\left(\frac{\omega_h}{T_h}\right) - \sinh\left(\frac{\omega_c}{T_c}\right) + \sinh\left(\frac{\omega_c}{T_c} - \frac{\omega_h}{T_h}\right) \right)}}. \quad (41)$$

Examining Eq. (41) shows that the Carnot limit is unattainable. When the Otto efficiency approached the Carnot limit $\frac{\omega_c}{\omega_h} = \frac{T_c}{T_h}$ the amplifiers efficiency becomes zero. This comparison between the two limits can be seen in Fig. 4.

The efficiency of Eq. (40) can be either smaller or greater than the Otto efficiency depending on the sign of G_2 . In the low temperature limit $G_2 < 0$, thus $\eta_o \leq \eta \leq \eta_c$. Increasing ϵ will increase the efficiency up to a critical point ϵ_{crit} which both both $G_1 \rightarrow 0$

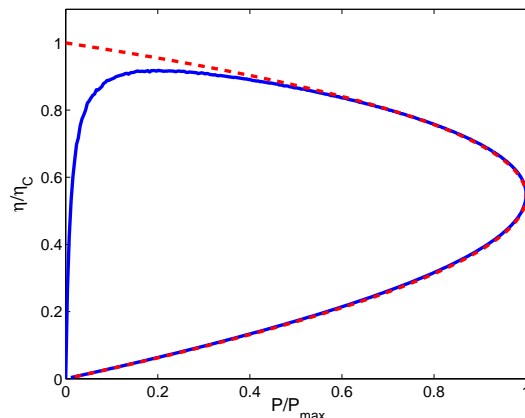


FIG. 4: The normalised efficiency η/η_c vs. the normalised power $\mathcal{P}/\mathcal{P}_{max}$ for fixed ϵ and Γ and ω_c while varying ω_h . The blue line is for finite Γ while the dashed red line is optimised at each point $\Gamma = 2\epsilon$. In this case $\epsilon \ll 1$.

and $G_2 \rightarrow 0$, since $N_{h(c)}^+ \rightarrow 0$ and $N_h^- \sim N_c^-$. At this point the engine operates at the Carnot limit and all currents vanish, such that the process becomes isoentropic, Cf. Fig. 5. In the high temperature limit for harmonic oscillators, while increasing ϵ , the gain G_2 will change sign and become positive, thus $\eta \leq \eta_o$, Cf. Fig. 6.

2. Optimizing the amplifier's performance

Further optimisation for power is obtained when the pumping rate Γ is optimised for maximum power then $\Gamma_{max} = 2\epsilon$ and the power becomes:

$$\mathcal{P} = -\frac{1}{2}\hbar\nu|\epsilon|G_1. \quad (42)$$

At the limit of high temperature and small ϵ the gain becomes $G_1 \approx \frac{K_B T_h}{\hbar\omega_h} - \frac{K_B T_c}{\hbar\omega_c}$, then optimising the power Eq. (42) with respect to the output frequency ν leads to:

$$\frac{\omega_c}{\omega_h} = \sqrt{\frac{T_c}{T_h}},$$

resulting in the efficiency at maximum power:

$$\eta_{CA} = 1 - \sqrt{\frac{T_c}{T_h}}, \quad (43)$$

which is the well established endoreversible result of Curzon and Ahlborn [2, 8]. The optimal power is obtained when all the characteristic parameters are balanced: $\epsilon \sim \Gamma \sim \kappa_c \sim \kappa_h$.

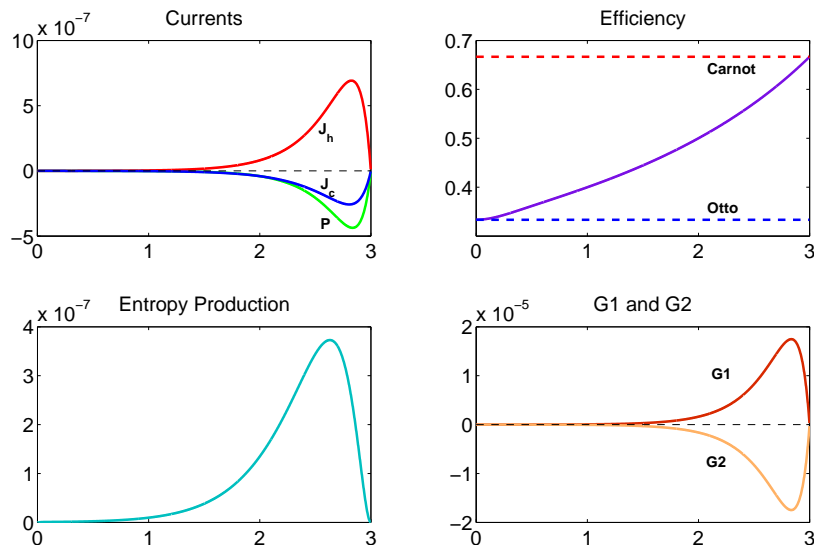


FIG. 5: Top left: The heat $\mathcal{J}_c, \mathcal{J}_h$ and power \mathcal{P} currents as a function of ϵ . Top Right: Efficiency η as a function of ϵ . Bottom left: Entropy production as a function of ϵ . Bottom right: The gain G_1 and G_2 as a function of ϵ . The harmonic tricycle engine operates in the limit of low temperature. $k_B T_c = 0.1$ and $k_B T_h = 0.3$, $\hbar\omega_c = 4$. and $\hbar\omega_h = 6$ and $\Gamma = 0.05$.

Figure 7 shows a trajectory of efficiency with respect to power with changing field coupling strength ϵ for different frequency ratios $\frac{\omega_c}{\omega_h} = \left(\frac{T_c}{T_h}\right)^\alpha$. The power vanishes with the coupling $\epsilon = 0$ and then when $\epsilon = \epsilon_{crit}$, at this point the splitting in the dressed energy levels nulls the gain.

D. Dynamical model of a 3-level engine

The dynamical description of the 3-level engine is closely related to the tricycle model [9]. The model is a template for the 3-level laser shown in Fig. 1 with inclusion of a dynamical description.

The Hamiltonian of the device has the form:

$$\hat{\mathbf{H}}_s = \hat{\mathbf{H}}_s^0 + \hat{\mathbf{V}}(t) = \begin{pmatrix} \epsilon_0 & 0 & 0 \\ 0 & \epsilon_1 & \epsilon e^{i\nu t} \\ 0 & \epsilon e^{-i\nu t} & \epsilon_2 \end{pmatrix} \quad (44)$$

where $\hat{\mathbf{H}}_s^0 = \sum \epsilon_i \hat{\mathbf{P}}_{ii}$, and $\hat{\mathbf{P}}_{ij} = |i\rangle\langle j|$. $\hat{\mathbf{V}}(t) = \epsilon (\hat{\mathbf{P}}_{12} e^{i\nu t} + \hat{\mathbf{P}}_{21} e^{-i\nu t})$. The state of the

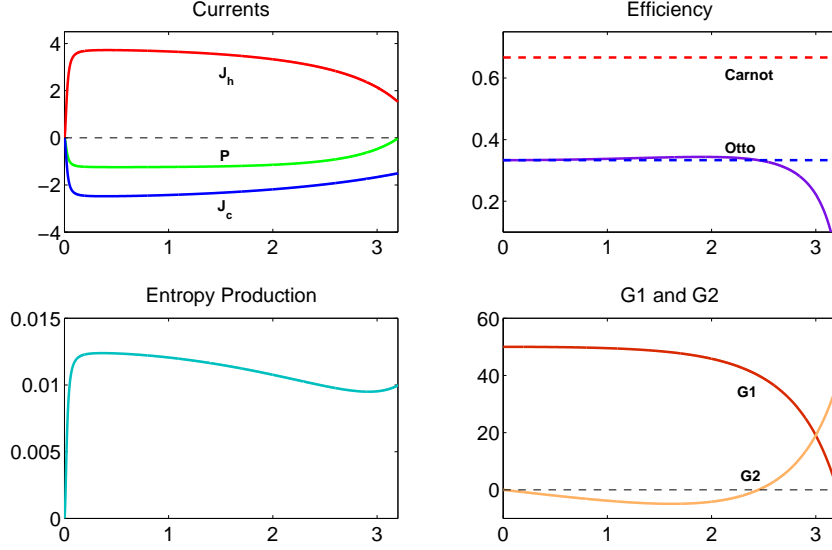


FIG. 6: Top left: The heat $\mathcal{J}_c, \mathcal{J}_h$ and power \mathcal{P} currents as a function of ϵ . Top Right: Efficiency η as a function of ϵ . Bottom left: Entropy production as a function of ϵ . Bottom right: The gain G_1 and G_2 as a function of ϵ . The harmonic tricycle engine operates in the limit of high temperature. $k_B T_c = 100$ and $k_B T_h = 300$, $\hbar\omega_c = 4$. and $\hbar\omega_h = 6$ and $\Gamma = 0.05$.

three-level system is fully characterised by the expectation values of any *eight* independent operators, excluding the identity operator. Different choices of the eight independent operators corresponds to different viewpoints.

- *The P representation*, is based on the eigen-representation of the *free* Hamiltonian, $\hat{\mathbf{H}}_s^0$, in the rotating frame.

$$\tilde{\mathbf{P}}_{i,j} = e^{-i\nu\hat{\mathbf{P}}_z t} \hat{\mathbf{P}}_{i,j} e^{i\nu\hat{\mathbf{P}}_z t} . \quad (45)$$

The following notations are also used [9]: $\hat{\mathbf{P}}_i = \hat{\mathbf{P}}_{ii}$, $\hat{\mathbf{P}}_+ = \hat{\mathbf{P}}_{21}$, $\hat{\mathbf{P}}_- = \hat{\mathbf{P}}_{12}$, $\hat{\mathbf{P}}_x = \frac{1}{2}(\hat{\mathbf{P}}_+ + \hat{\mathbf{P}}_-)$, $\hat{\mathbf{P}}_y = \frac{1}{2i}(\hat{\mathbf{P}}_+ - \hat{\mathbf{P}}_-)$, $\hat{\mathbf{P}}_z = \frac{1}{2}(\hat{\mathbf{P}}_u - \hat{\mathbf{P}}_1)$.

- *The Π representation*, which is the eigen-representation of the *full* Hamiltonian in the rotating frame, $\tilde{\mathbf{H}}_s = \hat{\mathbf{H}}_s^0 + \tilde{\mathbf{V}}$:

$$\tilde{\mathbf{\Pi}}_{i,j} = e^{-i\theta\tilde{\mathbf{P}}_y} \tilde{\mathbf{P}}_{i,j} e^{i\theta\tilde{\mathbf{P}}_y} , \quad (46)$$

where $\tan(\theta) = 2\epsilon/\Delta\omega$. Note that $\hat{\mathbf{H}}_s^0 + \tilde{\mathbf{V}} = \Delta\omega\hat{\mathbf{P}}_z + 2\epsilon\tilde{\mathbf{P}}_x = \nu\tilde{\mathbf{\Pi}}_z$ where $\Delta\omega = \omega_h - \omega_c - \nu$. Further notations are introduced by $\tilde{\mathbf{\Pi}}_i, \tilde{\mathbf{\Pi}}_{\pm}, \tilde{\mathbf{\Pi}}_x, \tilde{\mathbf{\Pi}}_y, \tilde{\mathbf{\Pi}}_z$, defined in a

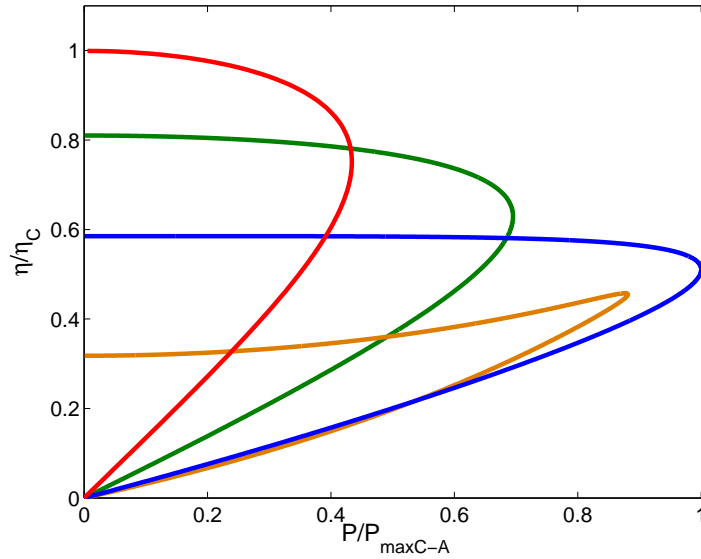


FIG. 7: The normalised efficiency η/η_c vs the normalised power $\mathcal{P}/\mathcal{P}_{max}$ for different optimal values of $\Gamma = 2\epsilon$. \mathcal{P}_{max} is obtained for the Curzon-Ahlborn ratio $\frac{\omega_c}{\omega_h} = \sqrt{\frac{T_c}{T_h}}$ shown in blue. The orange line is for $\frac{\omega_c}{\omega_h} = \left(\frac{T_c}{T_h}\right)^{1/4}$, the green line is for $\frac{\omega_c}{\omega_h} = \left(\frac{T_c}{T_h}\right)^{3/4}$. The red line is for the Carnot ratio $\frac{\omega_c}{\omega_h} \sim \frac{T_c}{T_h}$ where the power is multiplied by 10^3 .

similar manner to the analogous operators in the P representation, provided that each $\hat{\mathbf{P}}$ is replaced by a $\hat{\mathbf{\Pi}}$. The Π representation coincides with the atom-field dressed state representation [49]. This representation is employed to obtain the master equation for the engine [9].

The power and heat fluxes only depend on a reduced subset of $SU(2)$ operators, which are decoupled from the rest of the operators. As a result, the equations of motion of the 3-level amplifier can be represented by the set: $\tilde{\mathbf{P}}_+$, $\tilde{\mathbf{P}}_-$, $\tilde{\mathbf{P}}_u$, $\tilde{\mathbf{P}}_l$. The final equations of motion for these observables and the expressions for the power and efficiency become up to numerical factors identical to the expressions obtained for the driven quantum tricycle. Figure 8 shows a schematic view of the splitting of the energy levels of the 3-level system due to the driving field. As a result, the engine also splits into two parts, the upper and lower manifolds.

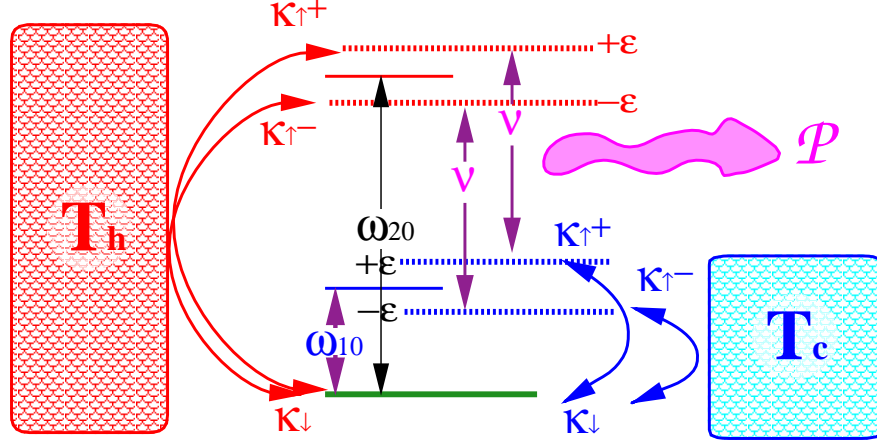


FIG. 8: The three-level-amplifier: The interaction with the external field splits the two upper levels. As a result the heat transport terms are modified. Two parallel engines emerge which can operated in opposite direction producing zero power for a certain choice of parameters.

1. The Generalized Lamb Equations in the P Representation

The basic equations describing the operation of a 3-level laser have been formulated by Lamb [50, 51]. These equations are modified to include the dynamical effects induced by the driving field. The equations of motion for the closed set of operators characterising the heat currents become:

$$\frac{d}{dt} \begin{pmatrix} \hat{\mathbf{P}}_+ \\ \hat{\mathbf{P}}_- \\ \hat{\mathbf{P}}_u \\ \hat{\mathbf{P}}_l \end{pmatrix} = \begin{pmatrix} i\Delta\omega + \Gamma_+ & 0 & -i\epsilon + \Gamma_{+u} & i\epsilon + \Gamma_{+l} \\ 0 & -i\Delta\omega + \Gamma_- & i\epsilon + \Gamma_{-u} & -i\epsilon + \Gamma_{-l} \\ -i\epsilon + \Gamma_{u+} & i\epsilon + \Gamma_{u-} & \Gamma_u & \Gamma_{ul} \\ i\epsilon + \Gamma_{l+} & -i\epsilon + \Gamma_{l-} & \Gamma_{lu} & \Gamma_l \end{pmatrix} \begin{pmatrix} \hat{\mathbf{P}}_+ \\ \hat{\mathbf{P}}_- \\ \hat{\mathbf{P}}_u \\ \hat{\mathbf{P}}_l \end{pmatrix} + \begin{pmatrix} \gamma_+ \\ \gamma_- \\ \gamma_u \\ \gamma_l \end{pmatrix} \quad (47)$$

The relaxation coefficients $\{\Gamma_{i,j}, \Gamma_i, \gamma_i\}$ consist of linear combinations of the bath parameters and can be found explicitly in Ref. [9].

The steady-state power and heat flows can be evaluated by solving the generalised Lamb equations. The results are represented by Eq. (36) where the definition of population is changed from that of a harmonic oscillator to a two-level-system: $N_{h(c)}^\pm = \frac{1}{e^{\beta_{h(c)}\omega_{h(c)}^\pm} + 1}$.

The numerator of the expressions for the power and heat flows consist of a sum of two contributions: one, which is proportional to the gain $N_h^+ - N_c^+$, is associated with the population inversion in the upper manifold, while the other, which is proportional to the gain $N_h^- - N_c^-$, is associated with the population inversion in the lower manifold.

At low temperature the 3-level amplifier model is equivalent to that of the harmonic tricycle. At the high temperature limit the gain G_2 is positive for all driving conditions ϵ . The maximum power point is the result of competition between the upper and lower manifolds. As ϵ increases, $N_h^+ - N_c^+$ increases, whereas $N_h^- - N_c^-$ decreases. Hence, the power production of the upper manifold increases, (i.e. becomes more negative) whereas that of the lower manifold decreases (i.e. becomes less negative).

From a thermodynamic point of view, each manifold is associated with a separate heat engine. As the coupling with the work reservoir (ϵ) increases, the engine associated with the upper manifold operates *faster* while that associated with the lower one operates *slower*. In addition, the energy is leaking from the former to the latter, thereby diminishing the net power production.

Not only does the power decrease as a function of ϵ , it also changes sign at a certain *finite* value of the field amplitude, denoted by ϵ_{crit} . This results from the fact that at some point the lower manifold starts operating backwards as a heat pump, rather than a heat engine. At $\epsilon = \epsilon_{crit}$, the power *consumption* by the lower manifold is exactly balanced by the power *production* of the upper manifold, such that the *net* power production is zero.

An examination of the steady-state heat fluxes, reveals that they do *not* vanish at zero-power operating conditions. Although both manifolds operate at the same rate and in opposite directions, the upper manifold absorbs more heat from the hot bath than that rejected by the lower one. Similarly, the upper manifold rejects more heat into the cold bath than that absorbed by the lower one. The net heat absorbed from the hot bath and rejected into the cold bath in zero-power operating conditions is therefore proportional to the difference in the energy gaps associated with these transitions. The entropy generated exclusively by the heat leak from the upper to lower manifold is obtained by eliminating the power in Eq. (39):

$$\frac{d}{dt}\Delta\mathcal{S}^l = \frac{\hbar\epsilon\Gamma G_2}{4k_B} \left(\frac{1}{T_c} - \frac{1}{T_h} \right) \geq 0. \quad (48)$$

Zero-power operating conditions correspond to the short circuit limit. Heat is effectively transferred *from* the hot bath *into* the cold bath, such that no net work is involved.

An interesting limit is that of low temperatures, such that $\hbar\epsilon/k_B \gg T_c, T_h$. This limit is realistic in the optical domain where $\nu \gg T_c, T_h$. In such a case $N_h^+ - N_c^+$ is negligible relative to $N_h^- - N_c^-$, and only the lower manifold needs be accounted for.

The value of ϵ_{crit} in this limit, denoted by ϵ_{crit}^{lT} , is that for which $N_h^- - N_c^- = 0$. It is

generally given by:

$$\epsilon_{crit}^{IT} = \frac{T_h \omega_c - T_c \omega_h}{T_h - T_c} . \quad (49)$$

The condition $T_h \omega_c - T_c \omega_h > 0$ is necessary and sufficient for lasing in the limit of weak driving fields. Population inversion becomes increasingly more difficult in this manifold as the field intensifies. It is therefore no longer a sufficient condition for lasing in intense driving fields. Finally, zero-power operating conditions in the low-temperature limit, obtained at $\epsilon = \epsilon_{crit}^{IT}$, asymptotically implies zero heat flows and hence the reversible limit. Indeed, substituting ϵ_{crit}^{IT} from Eq. (49) for ϵ reduces to the Carnot efficiency, $\eta_c = 1 - T_c/T_h$.

The difference between a 3-level-amplifier and the tricycle with harmonic oscillator filters at the high temperature limit is observed in Fig. 9. The source of the difference is the saturation of finite levels. The efficiency at maximum power is lower than the Curzon-Ahlborn efficiency approximated by:

$$\eta_{pmax} \approx \eta_c - \sqrt{\frac{k_B T_c}{\hbar \omega_h}} \eta_c^{\frac{1}{2}} . \quad (50)$$

E. The four-level engine and two-level engine

The four level-engine is a dynamical model of the 4-level laser [52]. In the four-level engine the pumping excitation step is isolated from the coupling to the external field by employing an additional cold reservoir. Figure 10 shows a schematic view of the structure of the engine. Analysing a static viewpoint, positive gain is obtained when

$$G = p_3 - p_2 = p_0 \left(e^{-\frac{\hbar \omega_h}{k_B T_h}} e^{\frac{\hbar \omega_{c2}}{k_B T_c}} - e^{-\frac{\hbar \omega_{c1}}{k_B T_c}} \right) \geq 0 , \quad (51)$$

where: $\omega_h = \omega_{30}$, $\omega_{c1} = \omega_{32}$, $\omega_{c2} = \omega_{10}$. The optimal output frequency at resonance is $\nu = \omega_h - \omega_{c1} - \omega_{c2}$, therefore the efficiency becomes: $\eta_o = \frac{\nu}{\omega_h}$. If the additional cold reservoir is assumed to have temperature T_c , then the Carnot restriction is obtained: $\eta_o \leq \eta_c$.

A dynamical analysis reveals a splitting of the energy levels that are driven by the external field, leading to a similar performance as the three-level amplifier. The advantage of the four-level engine is that the hot bath thermal pumping is isolated from the coupling to the power extraction, thus replacing the decoherence associated with the hot bath with a quieter operation associated with the cold bath. In addition, optimising performance by balancing the rates between the upper and lower manifold can be achieved by $\omega_{c1} = \omega_{c2}$.

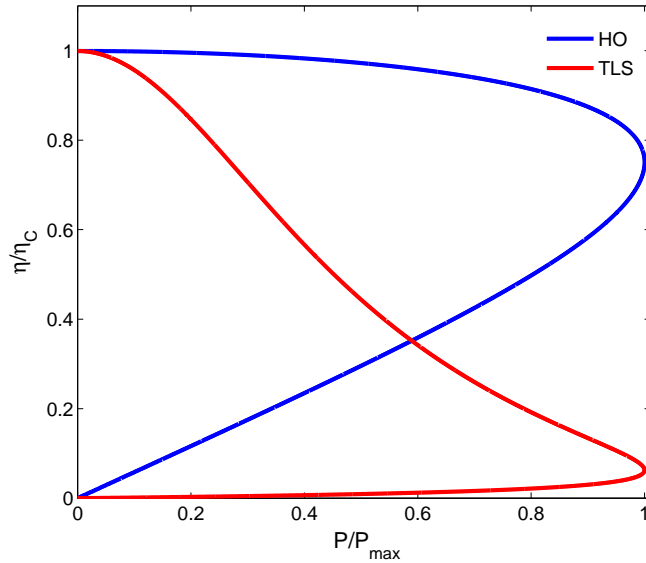


FIG. 9: The normalised efficiency η/η_c vs the normalised power $\mathcal{P}/\mathcal{P}_{max}$ for $\frac{\omega_c}{\omega_h} \sim \frac{T_c}{T_h}$ for varying $\Gamma = 2\epsilon$. The high temperature limit is shown where $\hbar\omega \ll k_b T$. The red line is the 3-level amplifier while the blue is the harmonic tricycle engine. Saturation limits the performance of the 3-level engine.

The four level engine has been employed to study the influence of initial coherence on the performance of the engine [53–59]. In this case the power output is connected to the two upper levels and the coherence is generated by splitting the ground state. The basic idea is that initial coherence present between energy levels associated with the entangling operator \hat{Y} , Eq. (35) can be exploited to generate additional power even from a single bath. There is no violation of the second-law since initial coherence reduces the initial entropy. Contact with a single bath will increase this entropy. A unitary manipulation can then exploit this entropy difference to generate work.

An extreme exploitation of the dynamical splitting of the energy levels due to the external driving field results in the two-level engine. Figure 11 sketches the schematic operation of the engine. Two excitations from the hot bath are required to generate a gain in the upper manifold. A clever choice of coupling to the bath is required to generate this gain. A model of such an engine has been worked out [60]. The maximum efficiency of such an engine becomes $\eta \leq \frac{1}{2} \leq \eta_c$ since two-pump steps are required for one output step.

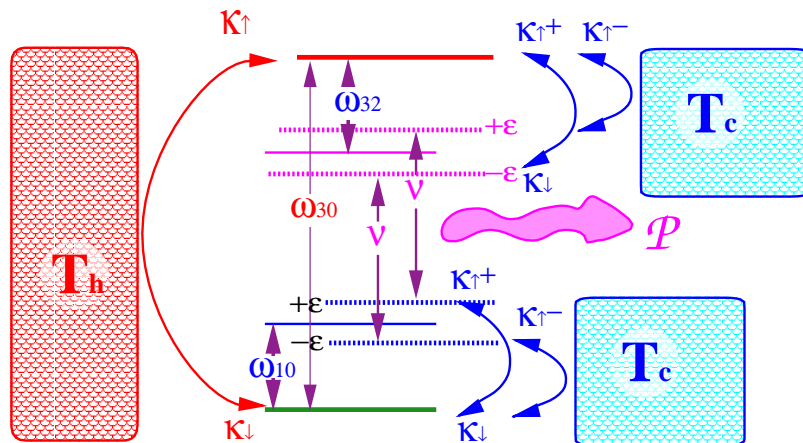


FIG. 10: The four-level-engine: The interaction with the external field splits the two upper levels. As a result the heat transport terms are modified. Two parallel engines emerge which can operated in opposite direction producing zero power for a certain choice of parameters. Coherence between levels 0 and 1 can enhance the performance by synchronising the engines. $\omega_h = \omega_{30}$, $\omega_{c1} = \omega_{32}$ and $\omega_{c2} = \omega_{10}$.

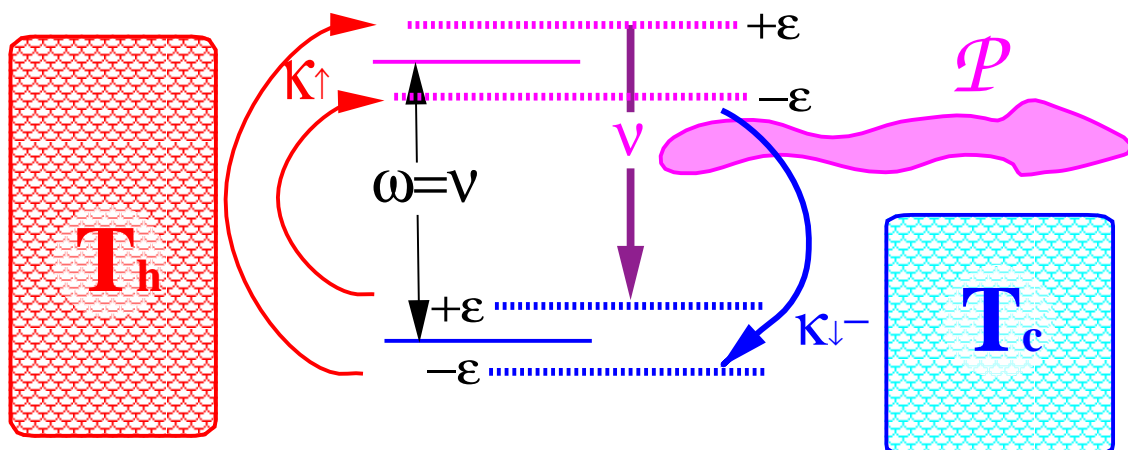


FIG. 11: The two-level-engine: The interaction with the external field splits the lower and upper levels. If the coupling to the hot and cold bath are engineered properly output power can be produced due to the positive gain between the upper split levels. Only the transitions leading to this mechanism are indicated.

F. Power storage

An integral part of an engine is a device which allows to store the power and retrieve it on demand, a flywheel. A model based on the tricycle of such a device just disconnects the

power bath and stores the energy in the power oscillator $\omega_w \hat{c}^\dagger \hat{c}$. Once there is positive gain generated by the hot and cold bath energy will flow to this oscillator. A model based on the 3-level amplifier suggested this approach [21, 35, 61]. The drawback of these studies is that they use a local description of the master equation. When the flywheel oscillator has large amplitude it will modify the system bath coupling in analogy to the dressed state picture [9].

Other studies also considered coupling to a cavity mode [57, 59, 62]. The issue to be addressed is the amount of energy that can be stored and then extracted. Since the storage mode is entangled to the rest of the engine this issue is delicate [62]. The amount of possible work to be extracted is defined by an entropy preserving unitary transformation to a passive state [63].

III. CONTINUOUS REFRIGERATORS

In a nutshell, refrigerators are just inverted heat engines. They employ power to pump heat from a cold to a hot bath. As in heat engines, the first and second law of thermodynamics imposes the same restrictions on the refrigerator's performance. The distinction between the static and dynamical viewpoints also applies. The key element in a refrigerator is entropy extraction and disposal. This entropy disposal problem is enhanced at low temperature where the entropy production in the cold bath can diverge. The unique feature of refrigerators is therefore the third-law of thermodynamics.

A. The third law of thermodynamics

Two independent formulations of the third-law of thermodynamics have been presented, both originally stated by Nernst [64–66]. The first is a purely static (equilibrium) one, also known as the "Nernst heat theorem", phrased:

- The entropy of any pure substance in thermodynamic equilibrium approaches zero as the temperature approaches zero.

The second formulation is known as the unattainability principle:

- It is impossible by any procedure, no matter how idealised, to reduce any assembly to absolute zero temperature in a finite number of operations [66, 67].

There is an ongoing debate on the relations between the two formulations and their relation to the second-law regarding which and if at all, one of these formulations implies the other [4, 68–70]. Quantum considerations can illuminate these issues. The tricycle model is the template used to analyse refrigerators performance as $T_c \rightarrow 0$.

We first analyse the implications of "Nernst heat theorem" and its relations to the second-law of thermodynamics. At steady state the second law implies that the total entropy production is non-negative, cf. Eq. (8):

$$\frac{d}{dt}\Delta S^{su} = -\frac{\mathcal{J}_c}{T_c} - \frac{\mathcal{J}_h}{T_h} - \frac{\mathcal{J}_w}{T_w} \geq 0 .$$

This behaviour can be quantified by a scaling exponent, as $T_c \rightarrow 0$ the cold current should scale with temperature as:

$$\mathcal{J}_c \propto T_c^{1+\alpha} ,$$

with an exponent α .

When the cold bath approaches the absolute zero temperature, it is necessary to eliminate the entropy production divergence at the cold side, when $T_c \rightarrow 0$ the entropy production scales as:

$$\Delta \dot{S}_c \sim -T_c^\alpha \quad , \quad \alpha \geq 0 . \quad (52)$$

For the case when $\alpha = 0$ the fulfilment of the second law depends on the entropy production of the other baths $-\frac{\mathcal{J}_h}{T_h} - \frac{\mathcal{J}_w}{T_w} > 0$, which should compensate for the negative entropy production of the cold bath. The first formulation of the third-law modifies this restriction. Instead of $\alpha \geq 0$ the third-law imposes $\alpha > 0$ guaranteeing that at absolute zero the entropy production at the cold bath is zero: $\Delta \dot{S}_c = 0$. Nernst's heat theorem then leads to the scaling condition of the heat current with temperature [11] :

$$\mathcal{J}_c \sim T_c^{\alpha+1} \quad \text{and} \quad \alpha > 0 . \quad (53)$$

We now examine the unattainability principle. Quantum mechanics enables a dynamical interpretation of the third-law modifying the definition to:

No refrigerator can cool a system to absolute zero temperature at finite time.

This form of the third-law is more restrictive, imposing limitations on the system bath interaction and the cold bath properties when $T_c \rightarrow 0$ [36]. To quantify the unattainability principle, the rate of temperature decrease of the cooling process should vanish according

to the characteristic exponent ζ :

$$\frac{dT_c(t)}{dt} = -c T_c^\zeta, \quad T_c \rightarrow 0 . \quad (54)$$

where c is a positive constant. Solving Eq. (54), leads to:

$$\begin{aligned} T_c(t)^{1-\zeta} &= T_c(0)^{1-\zeta} - ct & , \text{ for } \zeta < 1 , \\ T_c(t) &= T_c(0)e^{-ct} & , \text{ for } \zeta = 1 , \\ \frac{1}{T_c(t)^{\zeta-1}} &= \frac{1}{T_c(0)^{\zeta-1}} + ct & , \text{ for } \zeta > 1 , \end{aligned} \quad (55)$$

From Eq. (55) it is apparent that the cold bath can be cooled to zero temperature at finite time for $\zeta < 1$. The third-law requires therefore $\zeta \geq 1$. The two third-law scaling relations can be related by accounting for the heat capacity $c_V(T_c)$ of the cold bath:

$$\mathcal{J}_c(T_c(t)) = -c_V(T_c(t)) \frac{dT_c(t)}{dt} . \quad (56)$$

$c_V(T_c)$ is determined by the behaviour of the degrees of freedom of the cold bath at low temperature where $c_V \sim T_c^\eta$ when $T_c \rightarrow 0$. Therefore the scaling exponents are related $\zeta = 1 + \alpha - \eta$ [32].

The third-law scaling relations Eq. (56) and Eq. (53) can be used as an independent check for quantum refrigerator models [71]. Violation of these relations points to flaws in the quantum model of the device, typically in the derivation of the master equation.

B. The quantum power driven refrigerator

Laser cooling is a crucial technology for realising quantum devices. When the temperature is decreased, degrees of freedom freeze out and systems reveal their quantum character. Inspired by the mechanism of solid state lasers and their analogy with Carnot engines [6] it was realised that inverting the operation of the laser at the proper conditions will lead to refrigeration [72–75]. A few years later a different approach for laser cooling was initiated based on the doppler shift [76, 77]. In this scheme, translational degrees of freedom of atoms or ions were cooled by laser light detuned to the red of the atomic transition. Unfortunately the link to thermodynamics was forgotten. A flurry of activity then followed with the realisation that the actual temperature achieved were below the Doppler limit $k_B T_{\text{doppler}} = h\gamma/2$ where γ is the natural line width [78–80].

Elaborate quantum theories were devised to unravel the discrepancy. The recoil limit is based on the assumption that the photon momentum is in quasi equilibrium with the momentum of the atoms $\mathbf{p} = \hbar\mathbf{k}$. As a result, the temperature is related to the average kinetic energy:

$$k_B T_{recoil} = \frac{\hbar^2 k^2}{2M}, \quad (57)$$

where $\hbar k$ is the photon momentum and M the atomic mass of the particle being cooled. For sodium the doppler limit is $T_{doppler} = 235\mu K$ and the recoil limit $T_{recoil} = 2.39\mu K$ [81].

Thermodynamically, these limits do not bind, the only hard limit is the absolute zero $T_c = 0$. To approach this limit the cooling power has to be optimised to match the cold bath temperature. Unoptimised refrigerators become restricted by a minimum temperature above the absolute zero.

A reexamination of the elementary 3-level model stresses this point. Examining the heat engine model of Fig 1 shows that if the power direction is reversed a refrigerator is generated provided the gain is negative: $G = p_2 - p_1 < 0$. Assuming quasi equilibrium conditions. This leads to:

$$\frac{\omega_c}{\omega_h} = \frac{\omega_{10}}{\omega_{20}} \leq \frac{T_c}{T_h}, \quad (58)$$

which translated to a minimum temperature of $T_c(min) \geq \frac{\omega_c}{\omega_h} T_h$. We can consider typical values for laser cooling of Na based on the D line of 589.592 nm which translates to $\omega_h = 508.838 \cdot 10^{13} Hz$. If the translational cold bath is coupled to the hyperfine structure splitting $F_2 \rightarrow F_1$ of the ground state $3S_{1/2}$, meaning $\omega_c = 1.7716 \cdot 10^{10} Hz$. The cooling ratio becomes: $\frac{\omega_c}{\omega_h} = 3.48 \cdot 10^{-6}$ and the minimum temperature assuming room temperature of the hot bath is $T_c(min) \sim 1.510^{-3} K$. By employing a magnetic field the hyperfine levels F_1 split in three, leading to further splittings in the MHz limit increasing the cooling ratio by three orders of magnitude. When the cooling is in progress, the hyperfine splitting can be reduced by changing the magnetic field such that it follows the cold bath temperature. In principle any temperature above $T_c = 0$ is reachable.

C. Dynamical refrigerator models

A quantum dynamical framework of the refrigerator is based on the tricycle template. The work bath is replaced by a time dependent driving term. The cooling current can be calculated analytically. The derivation of the equation of motion are identical to the heat

engine model Sec. II C. The dynamical equations of the heat engine Eq. (36) converts to those of a refrigerator by inverting the sign of all heat currents. As a consequence the gain $G_1 \leq 0$, Eq. (37). For example, when $\epsilon > \kappa$ the cooling current becomes [36]:

$$\mathcal{J}_c = \frac{1}{2} \left(\hbar\omega_c^- \frac{\Gamma_c^- \Gamma_h^-}{\Gamma_c^- + \Gamma_h^-} (N_c^- - N_h^-) + \hbar\omega_c^+ \frac{\Gamma_c^+ \Gamma_h^+}{\Gamma_c^+ + \Gamma_h^+} (N_c^+ - N_h^+) \right). \quad (59)$$

The phenomena that the refrigerator splits into two parts is also found here. In a similar fashion the 3-level amplifier can be reversed to become a refrigerator [9]. The heat currents are identical to Eq. (36) with the TLS definition of $N_{c/h}^\pm$.

In a refrigerator the object of optimisation is the cooling power \mathcal{J}_c compared to the output power \mathcal{P} in an engine. The efficiency is defined by the coefficient of performance COP the ratio between \mathcal{J}_c and the input power \mathcal{P} .

$$COP = \frac{\mathcal{J}_c}{\mathcal{P}} \leq COP_o \leq COP_c \quad (60)$$

where $COP_o = \frac{\omega_c}{\nu}$ and $COP_c = \frac{T_c}{T_h - T_c}$. All power driven refrigerators are restricted by the Otto COP_o . In section III E the performance of power driven refrigerators at low temperature will be analysed.

D. The quantum absorption refrigerator

The absorption chiller is a refrigerator which employs a heat source to replace mechanical work for driving a heat pump [82]. The first device was developed in 1850 by the Carré brothers which became the first useful refrigerator. In 1926 Einstein and Szilárd invented an absorption refrigerator with no moving parts [83]. This fact is an inspiration for miniaturizing the device to solve the growing problem of heat generated in integrated circuits. Even a more challenging proposal is to miniaturize to the level of a few-level quantum system. Such a device could be incorporated into a quantum circuit. The first quantum version was based on the 3-level refrigerator [12] driven by thermal noise. A more recent model of an autonomous quantum absorption refrigerator with no external intervention based on three-qubits [37] has renewed interest in such devices. A setup of opto-mechanical refrigerators powered by incoherent thermal light was introduced by [84]. The study showed that cooling increases while increasing the photon number up to the point that fluctuation of the radiation pressure becomes dominant and heats the mechanical mode. Studies of cooling based

on electron tunneling were also considered. The working medium is composed of quantum dots [85, 86] or NIS junction [87] (Normal metal Insulator Superconductor). Heat is removed from the reservoir by electron transport which is induced by thermal or shot noise.

1. The 3-level absorption refrigerator

In the 3-level absorption refrigerator the power source has a finite temperature T_w . The coefficient of performance becomes $COP = \frac{\mathcal{J}_c}{\mathcal{J}_w}$. From the second and first law Eqs. (7), (8) using steady state conditions one obtains:

$$COP \leq \frac{(T_w - T_h)T_c}{(T_h - T_c)T_w} \quad (61)$$

and $T_w > T_h > T_c$ [82]. Under the assumption that the three baths are uncorrelated, the 3-level state is diagonal in the energy representation and determined by the heat conductivities [12, 88]. From these values the heat currents can be evaluated. This refrigerator emphasises the fact that no internal coherence is required for operation.

2. Tricycle absorption refrigerator

The template to understand the absorption refrigerator is the tricycle model, a refrigerator connected to three reservoirs with the Hamiltonian Eq. (5) and Eq. (6). A thermodynamical consistent description requires to first diagonalize the Hamiltonian and then to obtain the generalized master equations for each reservoir. The final step is to obtain the steady state heat currents \mathcal{J}_c , \mathcal{J}_h and \mathcal{J}_w . The nonlinearity in Eq. (6) hampers this task.

One remedy to this issue is to replace the harmonic oscillators in the model by qubits [38]. The other approach is to consider the high temperature limit of the power reservoir or a noise driven refrigerator [36, 89]. This three qubit refrigerator model was introduced as the ultimate miniaturization model [37, 90, 91]. The free Hamiltonian of the device has the form:

$$\hat{\mathbf{H}}_F = \hbar\omega_h \hat{\boldsymbol{\sigma}}_z^h + \hbar\omega_c \hat{\boldsymbol{\sigma}}_z^c + \hbar\nu \hat{\boldsymbol{\sigma}}_z^w \quad (62)$$

and the interaction Hamiltonian:

$$\hat{\mathbf{H}}_I = \hbar\epsilon \left(\hat{\boldsymbol{\sigma}}_+^h \otimes \hat{\boldsymbol{\sigma}}_-^c \otimes \hat{\boldsymbol{\sigma}}_-^w + \hat{\boldsymbol{\sigma}}_-^h \otimes \hat{\boldsymbol{\sigma}}_+^c \otimes \hat{\boldsymbol{\sigma}}_+^w \right), \quad (63)$$

where $\hat{\sigma}$ are two-level operators. Assuming $\omega_h = \omega_c + \nu$ the eigenstates of the Hamiltonian $\hat{\mathbf{H}} = \hat{\mathbf{H}}_F + \hat{\mathbf{H}}_I$ become:

Number	Energy	state	
1	0	$ 0, 0, 0\rangle$	
2	$\hbar\omega_c$	$ 0, 1, 0\rangle$	
3	$\hbar\nu$	$ 0, 0, 1\rangle$	
4	$\hbar(\nu + \epsilon)$	$\frac{1}{\sqrt{2}}(0, 1, 1\rangle + 1, 0, 0\rangle)$	(64)
5	$\hbar(\nu - \epsilon)$	$\frac{1}{\sqrt{2}}(0, 1, 1\rangle - 1, 0, 0\rangle)$	
6	$\hbar(\omega_c + \omega_h)$	$ 1, 1, 0\rangle$	
7	$\hbar(\omega_h + \nu)$	$ 1, 0, 1\rangle$	
8	$2\hbar\omega_h$	$ 1, 1, 1\rangle$	

The coupling to the bath has the form:

$$\hat{\mathbf{H}}_{SR} = \sum_{j=c,h} \lambda_j (\hat{\sigma}_+^j \otimes \hat{\mathbf{B}}_-^j + \hat{\sigma}_-^j \otimes \hat{\mathbf{B}}_+^j), \quad (65)$$

where j is the bath index. In this model, the coupling to the cold bath connects levels $1 \rightarrow 2$, $3 \rightarrow 4, 5$ and $4, 5 \rightarrow 8$. The master equation for the refrigerator can be derived using the weak system bath coupling limit [38]:

$$\mathcal{L} = \frac{i}{\hbar} [\hat{\mathbf{H}}, \bullet] + \mathcal{L}_h + \mathcal{L}_c + \mathcal{L}_w. \quad (66)$$

The cooling and power currents can be solved for this model. Of major importance is the distinction between the complete non-local description of the tricycle and a local description. In the local case the dissipative terms $\mathcal{L}_{h/c}$ are set to equilibrate only the local qubit. In the nonlocal case the local qubit is mixed with the other qubits due to the nonlinear coupling. As a result in the nonlocal approach it is impossible to reach the Carnot COP_c no matter how small is the internal coupling ϵ . This can be observed in Fig. 12, showing the COP vs the cooling current \mathcal{J}_c for different coupling strength ϵ . On the other hand the Carnot limit COP_c is reachable in the local model. An interesting observation is that a universal limit for the COP at the maximum cooling power was found [88] applicable for all absorption refrigerator modes of $COP^* \leq \frac{d}{d+1} COP_c$ where d is the dimensionality of the phonon cold bath.

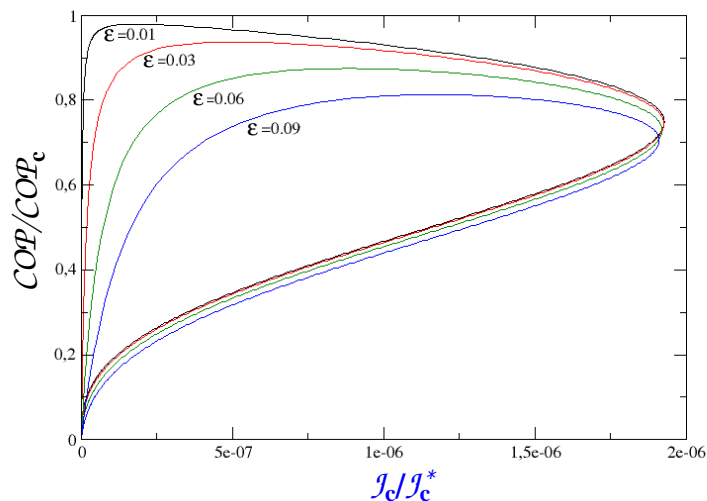


FIG. 12: The COP/COP_c of the 3-qubit refrigerator vs the normalised cold current J_c/J_c^* for different values of the internal coupling constant ϵ . The COP at maximum power is found to be bound by $3/4COP_c$ independent of ϵ . Figure in courtesy of L.A. Correa and J.P. Palao.

3. Noise driven refrigerator

An ideal power source generates zero entropy: $\Delta S_w = -\frac{J_w}{T_w}$. A pure mechanical external field achieves this goal. Another possibility is a thermal source, when $T_w \rightarrow \infty$ it also generates zero entropy. An unusual power source is noise. Gaussian white noise also carries with it zero entropy production. Analysis will show that the performance of refrigerators driven by all these power sources are very similar even when approaching the absolute zero temperature [89].

Employing the tricycle as a template we examine the option of employing noise as a power source. The simplest option is a Gaussian white noise source. As a result the interaction nonlinear term Eq. (6) is replaced with:

$$\hat{\mathbf{H}}_{int} = f(t) \left(\hat{\mathbf{a}}^\dagger \hat{\mathbf{b}} + \hat{\mathbf{a}} \hat{\mathbf{b}}^\dagger \right) = f(t) \hat{\mathbf{X}}, \quad (67)$$

where $f(t)$ is the noise field. $\hat{\mathbf{X}} = (\hat{\mathbf{a}}^\dagger \hat{\mathbf{b}} + \hat{\mathbf{a}} \hat{\mathbf{b}}^\dagger)$ is the generator of a swap operation between the two oscillators and is part of a set of $SU(2)$ operators, $\hat{\mathbf{Y}} = i(\hat{\mathbf{a}}^\dagger \hat{\mathbf{b}} - \hat{\mathbf{a}} \hat{\mathbf{b}}^\dagger)$, $\hat{\mathbf{Z}} = (\hat{\mathbf{a}}^\dagger \hat{\mathbf{a}} - \hat{\mathbf{b}}^\dagger \hat{\mathbf{b}})$ and the Casimir $\hat{\mathbf{N}} = (\hat{\mathbf{a}}^\dagger \hat{\mathbf{a}} + \hat{\mathbf{b}}^\dagger \hat{\mathbf{b}})$.

A Gaussian source of white noise is characterized by zero mean $\langle f(t) \rangle = 0$ and delta time correlation $\langle f(t)f(t') \rangle = 2\eta\delta(t-t')$. The Heisenberg equation for a time independent operator $\hat{\mathbf{O}}$ reduced to:

$$\frac{d}{dt}\hat{\mathbf{O}} = i[\hat{\mathbf{H}}_s, \hat{\mathbf{O}}] + \mathcal{L}_n^*(\hat{\mathbf{O}}) + \mathcal{L}_h^*(\hat{\mathbf{O}}) + \mathcal{L}_c^*(\hat{\mathbf{O}}), \quad (68)$$

where $\hat{\mathbf{H}}_s = \hbar\omega_h\hat{\mathbf{a}}^\dagger\hat{\mathbf{a}} + \hbar\omega_c\hat{\mathbf{b}}^\dagger\hat{\mathbf{b}}$. The noise dissipator for Gaussian noise is $\mathcal{L}_n^*(\hat{\mathbf{O}}) = -\eta[\hat{\mathbf{X}}, [\hat{\mathbf{X}}, \hat{\mathbf{O}}]]$ [48].

The next step is to derive the quantum Master equation of each reservoir. It is assumed that the reservoirs are uncorrelated and also uncorrelated with the driving noise. These conditions simplify the derivation of \mathcal{L}_h which become the standard energy relaxation terms, driving oscillator $\hbar\omega_h\hat{\mathbf{a}}^\dagger\hat{\mathbf{a}}$ to thermal equilibrium with temperature T_h and \mathcal{L}_c drives oscillator $\hbar\omega_c\hat{\mathbf{b}}^\dagger\hat{\mathbf{b}}$ to equilibrium T_c [92].

$$\begin{aligned} \mathcal{L}_h^*(\hat{\mathbf{O}}) &= \Gamma_h(N_h + 1) \left(\hat{\mathbf{a}}^\dagger\hat{\mathbf{O}}\hat{\mathbf{a}} - \frac{1}{2} \left\{ \hat{\mathbf{a}}^\dagger\hat{\mathbf{a}}, \hat{\mathbf{O}} \right\} \right) \\ &\quad + \Gamma_h N_h \left(\hat{\mathbf{a}}\hat{\mathbf{O}}\hat{\mathbf{a}}^\dagger - \frac{1}{2} \left\{ \hat{\mathbf{a}}\hat{\mathbf{a}}^\dagger, \hat{\mathbf{O}} \right\} \right) \\ \mathcal{L}_c^*(\hat{\mathbf{O}}) &= \Gamma_c(N_c + 1) \left(\hat{\mathbf{b}}^\dagger\hat{\mathbf{O}}\hat{\mathbf{b}} - \frac{1}{2} \left\{ \hat{\mathbf{b}}^\dagger\hat{\mathbf{b}}, \hat{\mathbf{O}} \right\} \right) \\ &\quad + \Gamma_c N_c \left(\hat{\mathbf{b}}\hat{\mathbf{O}}\hat{\mathbf{b}}^\dagger - \frac{1}{2} \left\{ \hat{\mathbf{b}}\hat{\mathbf{b}}^\dagger, \hat{\mathbf{O}} \right\} \right) \end{aligned} \quad (69)$$

The kinetic coefficients $\Gamma_{h/c}$ are determined from the system bath coupling and the spectral function [9, 36].

The equations of motion including the dissipative part are closed to the $SU(2)$ set of operators. To derive the cooling current $\mathcal{J}_c = \langle \mathcal{L}_c(\hbar\omega_c\hat{\mathbf{b}}^\dagger\hat{\mathbf{b}}) \rangle$, we solve for stationary solutions of $\hat{\mathbf{N}}$ and $\hat{\mathbf{Z}}$. The cooling current becomes:

$$\mathcal{J}_c = \hbar\omega_c \frac{2\eta\bar{\Gamma}}{2\eta+\Gamma} (N_c - N_h) \quad (70)$$

where the effective heat conductance is $\bar{\Gamma} = \frac{\Gamma_c\Gamma_h}{\Gamma_c+\Gamma_h}$. Cooling occurs for $N_c > N_h \Rightarrow \frac{\omega_h}{T_h} > \frac{\omega_c}{T_c}$. The coefficient of performance (COP) for the absorption chiller is defined by the relation $COP = \frac{\mathcal{J}_c}{\mathcal{J}_n}$, with the help of Eq. (70) we obtain the Otto COP_o [23], Cf. Eq. (60).

We now show the equivalence of the noise driven refrigerator with the high temperature limit of the work bath T_w . Based on the weak coupling limit the dissipative generator of the power bath becomes:

$$\begin{aligned} \mathcal{L}_w^*(\hat{\mathbf{O}}) &= \Gamma_w(N_w + 1) \left(\hat{\mathbf{a}}^\dagger\hat{\mathbf{b}}\hat{\mathbf{O}}\hat{\mathbf{b}}^\dagger\hat{\mathbf{a}} - \frac{1}{2} \left\{ \hat{\mathbf{a}}^\dagger\hat{\mathbf{a}}\hat{\mathbf{b}}\hat{\mathbf{b}}^\dagger, \hat{\mathbf{O}} \right\} \right) \\ &\quad + \Gamma_w N_w \left(\hat{\mathbf{a}}\hat{\mathbf{b}}^\dagger\hat{\mathbf{O}}\hat{\mathbf{a}}^\dagger\hat{\mathbf{b}} - \frac{1}{2} \left\{ \hat{\mathbf{a}}\hat{\mathbf{a}}^\dagger\hat{\mathbf{b}}^\dagger\hat{\mathbf{b}}, \hat{\mathbf{O}} \right\} \right) \end{aligned} \quad (71)$$

where $N_w = (\exp(\frac{\hbar\omega_w}{kT_h}) - 1)^{-1}$. At finite temperature $\mathcal{L}_w(\hat{\mathbf{O}})$ does not lead to a close set of equations. But in the limit of $T_w \rightarrow \infty$ it becomes equivalent to the Gaussian noise generator: $\mathcal{L}_w^*(\hat{\mathbf{O}}) = -\eta/2 \left([\hat{\mathbf{X}}, [\hat{\mathbf{X}}, \hat{\mathbf{O}}]] + [\hat{\mathbf{Y}}, [\hat{\mathbf{Y}}, \hat{\mathbf{O}}]] \right)$, where $\eta = \Gamma_w N_w$. This noise generator leads to the same current \mathcal{J}_c and COP as Eq. (70) and (60). We conclude that Gaussian noise represents the singular bath limit equivalent to $T_w \rightarrow \infty$.

Poisson white noise can be employed as a power source. This noise is typically generated by a sequence of independent random pulses with exponential inter-arrival times [93, 94]. These impulses drive the coupling between the oscillators in contact with the hot and cold bath leading to:

$$\begin{aligned} \frac{d\hat{\mathbf{O}}}{dt} = & (i/\hbar)[\tilde{\mathbf{H}}, \hat{\mathbf{O}}] - (i/\hbar)\lambda\langle\xi\rangle[\hat{\mathbf{X}}, \hat{\mathbf{O}}] \\ & + \lambda \left(\int_{-\infty}^{\infty} d\xi P(\xi) e^{(i/\hbar)\xi\hat{\mathbf{X}}} \hat{\mathbf{O}} e^{(-i/\hbar)\xi\hat{\mathbf{X}}} - \hat{\mathbf{O}} \right) , \end{aligned} \quad (72)$$

where $\tilde{\mathbf{H}}$ is the total Hamiltonian including the baths. λ is the rate of events and ξ is the impulse strength averaged over a distribution $P(\xi)$. Using the Hadamard lemma and the fact that the operators form a closed $SU(2)$ algebra, we can separate the noise contribution to its unitary and dissipation parts, leading to the master equation,

$$\frac{d\hat{\mathbf{O}}}{dt} = (i/\hbar)[\tilde{\mathbf{H}}, \hat{\mathbf{O}}] + (i/\hbar)[\hat{\mathbf{H}}', \hat{\mathbf{O}}] + \mathcal{L}_n^*(\hat{\mathbf{O}}) . \quad (73)$$

The unitary part is generated with the addition of the Hamiltonian $\hat{\mathbf{H}}' = \hbar\epsilon\hat{\mathbf{X}}$ and with the interaction

$$\epsilon = -\frac{\lambda}{2} \int d\xi P(\xi) (2\xi/\hbar - \sin(2\xi/\hbar)) . \quad (74)$$

This term can cause a direct heat leak from the hot to the cold bath. The noise generator $\mathcal{L}_n(\hat{\rho})$, can be reduced to the form $\mathcal{L}_n^*(\hat{\mathbf{O}}) = -\eta[\hat{\mathbf{X}}, [\hat{\mathbf{X}}, \hat{\mathbf{O}}]]$, with a modified noise parameter:

$$\eta = \frac{\lambda}{4} \left(1 - \int d\xi P(\xi) \cos(2\xi/\hbar) \right) . \quad (75)$$

The Poisson noise generates an effective Hamiltonian which is composed of $\tilde{\mathbf{H}}$ and $\hat{\mathbf{H}}'$, modifying the energy levels of the working medium. This new Hamiltonian structure has to be incorporated in the derivation of the master equation otherwise the second law will be violated. The first step is to rewrite the system Hamiltonian in its dressed form. A new set of bosonic operators is defined

$$\begin{aligned} \hat{\mathbf{A}}_1 &= \hat{\mathbf{a}} \cos(\theta) + \hat{\mathbf{b}} \sin(\theta) \\ \hat{\mathbf{A}}_2 &= \hat{\mathbf{b}} \cos(\theta) - \hat{\mathbf{a}} \sin(\theta) , \end{aligned} \quad (76)$$

The dressed Hamiltonian is given by:

$$\hat{\mathbf{H}}_s = \hbar\Omega_+ \hat{\mathbf{A}}_1^\dagger \hat{\mathbf{A}}_1 + \hbar\Omega_- \hat{\mathbf{A}}_2^\dagger \hat{\mathbf{A}}_2, \quad (77)$$

where $\Omega_\pm = \frac{\omega_h + \omega_c}{2} \pm \sqrt{(\frac{\omega_h - \omega_c}{2})^2 + \epsilon^2}$ and $\cos^2(\theta) = \frac{\omega_h - \Omega_-}{\Omega_+ - \Omega_-}$ Eq.(77) impose the restriction, $\Omega_\pm > 0$ which can be translated to $\omega_h \omega_c > \epsilon^2$. The master equation in the Heisenberg representation becomes:

$$\frac{d\hat{\mathbf{O}}}{dt} = (i/\hbar)[\hat{\mathbf{H}}_s, \hat{\mathbf{O}}] + \mathcal{L}_h^*(\hat{\mathbf{O}}) + \mathcal{L}_c^*(\hat{\mathbf{O}}) + \mathcal{L}_n^*(\hat{\mathbf{O}}), \quad (78)$$

where the details can be found in ref [36]. The noise generator becomes:

$$\mathcal{L}_n^*(\hat{\mathbf{O}}) = -\eta[\hat{\mathbf{W}}, [\hat{\mathbf{W}}, \hat{\mathbf{O}}]], \quad (79)$$

where $\hat{\mathbf{W}} = \sin(2\theta)\hat{\mathbf{Z}} + \cos(2\theta)\hat{\mathbf{X}}$. Again, the $SU(2)$ algebra is employed to define the operators: $\hat{\mathbf{X}} = (\hat{\mathbf{A}}_1^\dagger \hat{\mathbf{A}}_2 + \hat{\mathbf{A}}_2^\dagger \hat{\mathbf{A}}_1)$, $\hat{\mathbf{Y}} = i(\hat{\mathbf{A}}_1^\dagger \hat{\mathbf{A}}_2 - \hat{\mathbf{A}}_2^\dagger \hat{\mathbf{A}}_1)$ and $\hat{\mathbf{Z}} = (\hat{\mathbf{A}}_1^\dagger \hat{\mathbf{A}}_1 - \hat{\mathbf{A}}_2^\dagger \hat{\mathbf{A}}_2)$. The total number of excitations is accounted for by the operator $\hat{\mathbf{N}} = (\hat{\mathbf{A}}_1^\dagger \hat{\mathbf{A}}_1 + \hat{\mathbf{A}}_2^\dagger \hat{\mathbf{A}}_2)$.

Once the set of linear equations is solved the exact expression for the heat currents is extracted, $\mathcal{J}_h = \langle \mathcal{L}_h^*(\hat{\mathbf{H}}_s) \rangle$, $\mathcal{J}_c = \langle \mathcal{L}_c^*(\hat{\mathbf{H}}_s) \rangle$ and $\mathcal{J}_n = \langle \mathcal{L}_n^*(\hat{\mathbf{H}}_s) \rangle$.

The distribution of impulse determines the performance of the refrigerator. For a normal distribution of impulses in Eq. (72), $P(\xi) = \frac{1}{\sqrt{2\pi\sigma^2}} e^{-\frac{(\xi - \xi_0)^2}{2\sigma^2}}$. The energy shift is controlled by:

$$\epsilon = -\frac{\lambda}{2}(2\xi_0/\hbar - e^{-\frac{2\sigma^2}{\hbar^2}} \sin(2\xi_0/\hbar)). \quad (80)$$

The effective noise strength becomes:

$$\eta = \frac{\lambda}{4}(1 - e^{-\frac{2\sigma^2}{\hbar^2}} \cos(2\xi_0/\hbar)). \quad (81)$$

In the limit of $\sigma \rightarrow 0$, $P(\xi) = \delta(\xi - \xi_0)$. Another possibility is an exponential distribution: $P(\xi) = \frac{1}{\xi_0} e^{-\frac{\xi}{\xi_0}}$ then:

$$\epsilon = -\lambda \frac{(\xi_0/\hbar)^3}{4(1 + (\xi_0/\hbar)^2)} \quad (82)$$

and

$$\eta = \lambda \frac{(\xi_0/\hbar)^2}{1 + 4(\xi_0/\hbar)^2}. \quad (83)$$

The Poissonian noise plays two opposing roles. On the one hand it increases the cooling current \mathcal{J}_c , by increasing η . On the other hand it decreases ϵ (becomes more negative) and by

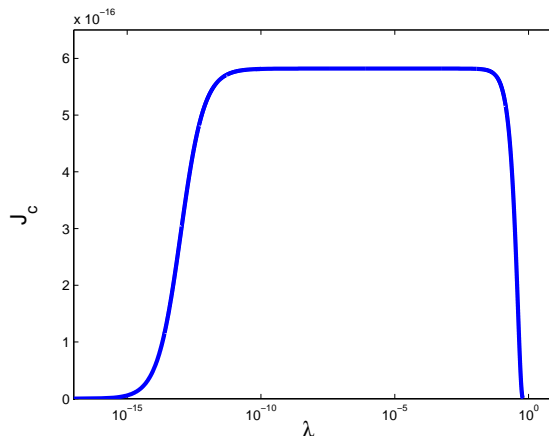


FIG. 13: The noise driven refrigerator. The cooling current \mathcal{J}_c as a function of λ . The refrigerator is powered by a Poissonian noise source. The plot is for the limit of $\sigma \rightarrow 0$.

that decreases \mathcal{J}_c . Both parameters η and ϵ depend linearly on λ , which can be interpreted as the rate of photon absorption in the system which enhances the cooling process. Fig. 13 shows that \mathcal{J}_c increases with λ until a point where ϵ dominates and \mathcal{J}_c decreases.

The *COP* for the Poisson driven refrigerator is restricted by the Otto and Carnot *COP*:

$$COP = \frac{\Omega_-}{\Omega_+ - \Omega_-} \leq \frac{\omega_c}{\omega_h - \omega_c} \leq \frac{T_c}{T_h - T_c}. \quad (84)$$

E. Refrigerators operating close to the limit $T_c \rightarrow 0$ and the third-law of thermodynamics

The performance of all types of refrigerators at low temperature have universal properties. In the power driven refrigerators the lower split manifold is dominant, leading to the cold current:

$$\mathcal{J}_c \approx \hbar\omega_c^- \frac{2\epsilon^2\bar{\Gamma}}{4\epsilon^2 + \Gamma_c\Gamma_h} \cdot G, \quad (85)$$

where the gain $G = N_c^- - N_h^-$ and $\bar{\Gamma} = \frac{\Gamma_c\Gamma_h}{\Gamma_c + \Gamma_h}$.

In the 3-level absorption refrigerator the cold current becomes [88]:

$$\mathcal{J}_c = \hbar\omega_c \frac{\Gamma_c\Gamma_h\Gamma_w}{\Delta} \cdot G \quad (86)$$

where Δ is a combination of kinetic constants and $G = e^{-\frac{\hbar\omega_w}{k_B T_w}} e^{-\frac{\hbar\omega_c}{k_B T_c}} - e^{-\frac{\hbar\omega_h}{k_B T_h}}$.

In the Guassian noise driven refrigerator Eq. (70) becomes:

$$\mathcal{J}_c = \hbar\omega_c \frac{2\eta\bar{\Gamma}}{2\eta + \Gamma} \cdot G. \quad (87)$$

where $G = N_c - N_h$.

In the Poisson driven refrigerator we obtain:

$$\mathcal{J}_c \approx \hbar \Omega_- \frac{2\eta \bar{\Gamma}}{2\eta + \bar{\Gamma}} \cdot G, \quad (88)$$

with $G = (N_c^- - N_h^+)$ and $\Omega_- \approx \omega_c - \frac{\epsilon^2}{\omega_h - \omega_c}$. All expressions for the cooling current \mathcal{J}_c are a product of an energy quant $\hbar\omega_c$, the effective heat conductance and the gain G .

To approach the absolute zero temperature a further optimisation is required. Optimising the gain G is obtained when $\omega_h \rightarrow \infty$, which leads to $G \sim e^{-\frac{\hbar\omega_c}{k_B T_c}}$. In addition the driving amplitude should be balanced with the heat conductivity. The cooling current can also be expressed in terms of the relaxation rate to the bath via the relation $\gamma(\omega)e^{-\frac{\hbar\omega}{k_B T}} = \Gamma(\omega)N(\omega)$. The universal optimised cooling current as $T_c \rightarrow 0$ becomes:

$$\mathcal{J}_c = \hbar\omega_c \cdot \gamma_c \cdot e^{-\frac{\hbar\omega_c}{k_B T_c}}. \quad (89)$$

This form is correct both in the weak coupling limit and the low density limit. The heat current \mathcal{J}_c can be interpreted as the quant of energy $\hbar\omega_c$ extracted from the cold bath at the rate γ_c multiplied by a Boltzmann factor. Further optimisation with respect to ω_c is dominated by the exponential Boltzmann factor (Optimising the function $x^a e^{-x/b}$ leads to $x^* \propto b$). As a result $\omega_c^* \propto T_c$, obtaining: $\mathcal{J}_c \propto \omega_c^* \cdot \gamma_c(\omega_c^*)$. The linear relation between the optimal frequency ω_c and T_c allows to translate the temperature scaling relations to the low frequency scaling relations of $\gamma_c(\omega) \sim \omega^\mu$ and $c_V(\omega) \sim \omega^\eta$ when $\omega \rightarrow 0$.

To fulfil "Nernst's heat theorem" Eq. (53), the scaling of the relaxation rate is restricted to $\gamma_c(\omega) \sim \omega^\alpha$ and $\alpha > 0$. The fulfilment of the unattainability principle Eq. (56) depends on the ratio between the relaxation rate and the heat capacity $\gamma_c/c_V \sim \omega^{\zeta-1}$ where $\zeta > 1$.

The low frequency properties of the relaxation rate γ_c and the heat capacity c_V are examined. For three-dimensional ideal degenerate Bose gases c_V scales as $T_c^{3/2}$. For degenerate Fermi gas c_V scales as T_c . In both cases the fraction of the gas that can be cooled decreases with temperature. Based on a collision model when cooling occurs due to inelastic scattering we have found the scaling exponent $\zeta = 3/2$ for both Bose and Fermi degenerate gas [36].

The most studied generic bath is the harmonic bath. It includes the electromagnetic field: (a photon bath), or a macroscopic piece of solid; (a phonon bath), or Bogoliubov excitations in a Bose-Einstein condensate. The standard form of the bath's Hamiltonian is:

$$\hat{\mathbf{H}}_{int} = (\hat{\mathbf{b}} + \hat{\mathbf{b}}^\dagger) \left(\sum_k (g(k)\hat{\mathbf{a}}(k) + \bar{g}(k)\hat{\mathbf{a}}^\dagger(k)) \right), \quad \hat{\mathbf{H}}_B = \sum_k \omega(k)\hat{\mathbf{a}}^\dagger(k)\hat{\mathbf{a}}(k) \quad (90)$$

where $\hat{\mathbf{a}}(k)$ and $\hat{\mathbf{a}}^\dagger(k)$ are the annihilation and creation operators for a mode k . For this model, the weak coupling limit procedure leads to the GKS-L generator with the cold bath relaxation rate given by [36]:

$$\gamma_c \equiv \gamma_c(\omega_c) = \pi \sum_k |g(k)|^2 \delta(\omega(k) - \omega_c) \left[1 - e^{-\frac{\hbar\omega(k)}{k_B T_c}} \right]^{-1}. \quad (91)$$

For the bosonic field in d -dimensional space, with the linear low-frequency dispersion law ($\omega(k) \sim |k|$), the following scaling properties for the cooling rate at low frequencies are obtained: $\gamma_c \sim \omega_c^\kappa \omega_c^{d-1}$ where ω_c^κ represents the scaling of the form-factor $|g(\omega)|^2$, and ω_c^{d-1} is the scaling of the density of modes. For $\omega_c \sim T_c$, the final current scaling becomes: $\mathcal{J}_c^{opt} \sim T_c^{d+\kappa}$ or $\alpha = d + \kappa - 1$.

At low temperatures, the heat capacity of the bosonic systems scales like: $c_V(T_c) \sim T_c^d$, which produces the scaling $\zeta = \kappa$. This means that to fulfil the third law $\kappa \geq 1$. To rationalise the scaling, c_V is a volume property and γ_c is a surface property, so $\omega_c \gamma_c$ scales the same as c_V . The scaling of the form factor κ is related to the speed the excitation can be carried away from the surface.

The exponent $\kappa = 1$ when $\omega \rightarrow 0$, is typical in systems such as electromagnetic fields or acoustic phonons which have linear dispersion law, $\omega(k) = v|k|$. In these cases the form-factor becomes, $g(k) \sim |k|/\sqrt{\omega(k)}$, therefore $|g(\omega)|^2 \sim |k|$. The condition $\kappa \geq 1$ excludes exotic dispersion laws, $\omega(k) \sim |k|^\delta$ with $\delta < 1$, which produce infinite group velocity forbidden by relativity theory. Moreover, the popular choice of Ohmic coupling is excluded for systems in dimension $d > 1$ [32]. We should mention that challenges to the third law have been published [95]. Our viewpoint is that these discrepancies are the result of flaws in reduction of the spin bath to a harmonic spectral density formulation.

IV. SUMMARY

Thermodynamics represents physical reality with an amazingly small number of variables. In equilibrium, the energy operator $\hat{\mathbf{H}}$ is sufficient to reconstruct the state of the system, from which all other observables can be deduced. Dynamical systems out of equilibrium require more variables. Quantum thermodynamics advocates that only a few additional variables are required to describe a quantum device; a heat engine or a refrigerator. A description based on Heisenberg equation of motion lends itself to this viewpoint. A sufficient condition

for the set of operators to be closed to the Hamiltonian is that they form a Lie algebra. In addition the Hamiltonian needs to be a linear combination of operators from the same algebra [96]. Finally, the operators have to be closed to the dissipative part $\mathcal{L}_{h/c}$. Most of the solvable models in this review were based on the SU(2) Lie algebra with four operators. We can chose them to represent the energy $\hat{\mathbf{H}}$, the identity $\hat{\mathbf{I}}$, and two additional operators $\hat{\mathbf{X}}$ and $\hat{\mathbf{Y}}$. These operators can associate with coherence since $[\hat{\mathbf{H}}, \hat{\mathbf{X}}] \neq 0$, $[\hat{\mathbf{H}}, \hat{\mathbf{Y}}] \neq 0$. Generically in these models the power is proportional to the coherence $\mathcal{P} \propto \langle \hat{\mathbf{Y}} \rangle$. We can speculate that steady state operation of a working engine or refrigerator is minimally characterised by the SU(2) algebra of three non commuting operators. This is also the case in reciprocating engines [97–99].

The Hamiltonian can be decomposed to non-commuting local operators which couple to the baths. The non-local structure influences the derivation of the master equation. A local approach based on equilibrating $\hat{\mathbf{H}}_s$ leads to equations of motion that can violate the second-law of thermodynamics [9, 32, 36, 71]. A thermodynamically consistent derivations requires a pre-diagonalization of the system Hamiltonian. This Hamiltonian defines the system-bath weak coupling approximation leading to the GKS-L completely positive generator.

Quantum mechanics introduces dynamics into thermodynamics. As a result the laws of thermodynamics have to be reformulated, replacing heat to heat currents and work to power. The first law at steady state requires that the sum of these currents is zero. For the devices considered, the entropy production is exclusively generated in the baths and the sum of all contributions is positive. All quantum devices should be consistent with the first and second laws of thermodynamics. Apparent violations point to erroneous derivations of the dynamical equations of motion.

The tricycle template is a universal description for continuous quantum heat engines and refrigerators. This model incorporates basic thermodynamic ideas within a quantum formalism. The tricycle combines three energy currents from three sources by a nonlinear interaction. A nonlinear construction is the minimum requirement for all heat engines or refrigerators. This universality means that the same structure can describe a wide range of quantum devices. The performance characteristics are given by the choice of working medium and reservoirs. In the derivation, the reservoirs are characterised by their temperature and correlation functions. The working medium filters out the channels of heat transfer and power.

The tradeoff between power and efficiency is a universal characteristic of the quantum devices. The output power or the cooling current exhibit a turnover with any control parameter [100]. For example, when the coupling parameter to the external field is increased first the power or cooling current increase with it, but then beyond a critical parameter, due to splitting of the energy levels a decrease in performance appears. Another turnover phenomena is observed when the coupling parameter to the baths is increased. Initially increasing the coupling will allow more heat to flow to the device. Above a critical value dissipation will degrade the coherence and with it the performance. Optimal power and optimal cooling currents are obtained in a balanced operational point, far from reversible conditions of maximum efficiency.

The quantum version of the third law originates from the existence of a ground state. The third law can be thought of as a limit to the distillation of a pure ground state in a subsystem disentangling it from the environment. We can generalize and apply the third law to any pure state of the subsystem since such a state is accessible from the ground state by a unitary transformation. Unitary transformations are isoentropic and therefore allowed by the Nernst heat theorem at $T_c = 0$. The quantum dilemma of cooling to a pure state stems from the fact that a system-bath interaction is required to induce a change of entropy of the system. However, such an interaction generates system-bath entanglement so that the system cannot be in a pure state. Approaching the absolute zero temperature is a delicate manoeuvre. The system-bath coupling has to be reduced while the cooling takes place, eventually vanishing when $T_c \rightarrow 0$. As a result the means to cool are exhausted before the target is reached [101, 102]. The universal behaviour of all quantum refrigerators as $T_c \rightarrow 0$ emphasises this point.

How do quantum phenomena such as coherence and entanglement influence performance? This issue can be separated into global effects which include the reservoirs and internal quantum effects within the device. The description of the heat transport into the device by the GKS-L Master equation is the thermodynamic equivalent of an isothermal partition. In this description the system and bath are not entangled [32]. The issue of internal quantum effects is more subtle. Internal coherence is necessary for operation in quantum driven devices. For quantum autonomous absorption refrigerators it has been recently claimed that, although present, coherence is not determinant in the engine operation [88]. Other papers claim the opposite [53, 86, 103]. Entanglement has been related to extraction of

additional work [62, 104, 105]. These issues require further study.

For completeness we would like to mention what was excluded from the present review: Reciprocating heat engines and refrigerators. Significant insight can be gained from the analysis of such devices. The template is the quantum Otto four stroke cycle where the unitary adiabatic branches are separated from the heat transport [22–24, 34, 99, 106–111]. The analysis of reciprocating engine is simplified due to this separation. The disadvantage is that the timing of the branches is determined externally. The review of reciprocating engines and refrigerators will be treated in a separate publication.

Finally, we can conclude from this review that quantum devices when analysed according to the laws of quantum mechanics are consistent with a dynamical interpretation of the laws of thermodynamics.

a. Acknowledgments: This review was supported by the Israel Science Foundation. We want to thank Tova Feldmann, Eitan Geva, Jose P. Palao, Jeff Gordon, Lajos Diosi, Peter Salamon, Gershon Kuritzky and Robert Alicki for sharing their wisdom.

-
- [1] Carnot S. 1824. *Réflexions sur la Puissance Motrice du Feu et sur les Machines propres à Développer cette Puissance*. Paris: Bachelier
- [2] Curzon F, Ahlborn B. 1975. Efficiency of a carnot engine at maximum power output. *Am. J. Phys.* 43:22
- [3] Salamon P, Nulton J, Siragusa G, Andersen TR, Limon A. 2001. Principles of control thermodynamics. *Energy* 26:307–319
- [4] Landsberg PT. 1956. Foundations of thermodynamics. *Rev. Mod. Phys.* 28:363
- [5] Einstein A. 1905. "über einen die erzeugung und verwandlung des lichtes betreffenden heuristischen gesichtspunkt (on a heuristic viewpoint concerning the production and transformation of light)". *Annalen der Physik* 17:132
- [6] Geusic J, Schulz-DuBios E, Scovil H. 1959. Three-level masers as heat engines. *Phys. Rev. Lett.* 2:262
- [7] Geusic J, du Bois EOS, Grasse RD, Scovil HE. 1967. Quantum equivalence of the carnot cycle. *Phys. Rev.* 156:343
- [8] Kosloff R. 1984. A Quantum Mechanical Open System as a Model of a Heat Engine. *J. Chem. Phys.* 80:1625–1631
- [9] Geva E, Kosloff R. 1996. The Quantum Heat Engine and Heat Pump: An Irreversible Thermodynamic Analysis of The Three-Level Amplifier. *J. Chem. Phys.* 104:7681–7698
- [10] Partovi M. 1989. Quantum thermodynamics. *Physics Letters A* 137:440
- [11] Kosloff R, Geva E, Gordon JM. 2000. The quantum refrigerator in quest of the absolute zero. *J. Appl. Phys.* 87:8093–8097
- [12] Palao JP, Kosloff R, Gordon JM. 2001. Quantum thermodynamic cooling cycle. *Phys. Rev. E* 64:056130–8
- [13] Lloyd S. 1997. Quantum-mechanical maxwells demon. *Phys. Rev. A* 56:3374
- [14] He J, Chen J, Hua B. 2002. Quantum refrigeration cycles using spin- $\frac{1}{2}$ systems as working substance. *Phys. Rev. E* 65:036145
- [15] Lieb EH, Yngvason J. 1999. The physics and mathematics of the second law of thermodynamics. *Phys. Rev.* 310:1
- [16] Bender CM, Brody DC, Meister BK. 2002. Entropy and temperature of a quantum carnot

- engine. *Proceedings of the Royal Society of London. Series A: Mathematical, Physical and Engineering Sciences* 458:1519
- [17] Kieu TD. 2004. The second law, maxwell's demon, and work derivable from quantum heat engines. *Phys. Rev. Lett.* 93:140403
- [18] Segal D, Nitzan A. 2006. Molecular heat pump. *Phys. Rev. E* 73:026109
- [19] Bushev P, Rotter D, Wilson A, Dubin F, Becher C, et al. 2006. Feedback cooling of a single trapped ion. *Phys. Rev. Lett.* 96:60010
- [20] Quan HT, Liu YX, Sun CP, Nori F. 2007. Quantum thermodynamic cycles and quantum heat engines. *Phys. Rev. E* 76:031105
- [21] Boukobza E, Tannor DJ. 2008. Thermodynamic analysis of quantum light purification. *Phys. Rev. A* 78:013825
- [22] Birjukov J, Jahnke T, Mahler G. 2008. Quantum thermodynamic processes: a control theory for machine cycles. *Eur. Phys. J. B* 64:105
- [23] Jahnke T, Birjukov J, Mahler G. 2008. On the nature of thermodynamic extremum principles: The case of maximum efficiency and maximum work. *Ann.Phys.* 17:88
- [24] Allahverdyan AE, Johal RS, Mahler G. 2008. Work extremum principle: Structure and function of quantum heat engines. *Phys. Rev. E* 77:041118
- [25] Segal D. 2009. Vibrational relaxation in the kubo oscillator: Stochastic pumping of heat. *J. Chem. Phys.* 130:134510
- [26] Wang H, Liu S, He J. 2009. Thermal entanglement in two-atom cavity QED and the entangled quantum otto engine. *Phys. Rev. E* 79:041113
- [27] Maruyama K, Nori F, Verdal V. 2009. Colloquium: The physics of Maxwell's demon and information. *Rev. Mod. Phys.* 81:1
- [28] Beneti G, Casati G, Prosen T, Saito K. 2013. Colloquium: Funduamental aspects of steady state heat to work conversion. *Rev. Mod. Phys.* to appear.
- [29] Gemmer J, Michel M, Mahler G. 2009. *Quantum Thermodynamics*. Springer
- [30] Olshanii M. 2012. Geometry of quantum observables and thermodynamics of small systems. *ArXiv e-prints:1208.0582*
- [31] Anders J, Giovannetti V. 2013. Thermodynamics of discrete quantum processes. *New Jour. of Phys.* 15:033022
- [32] Kosloff R. 2013. Quantum Thermodynamics: A Dynamical Viewpoint. *Entropy* 15

- [33] Mandal D, Quan HT, Jarzynski C. 2013. Maxwells Refrigerator: An Exactly Solvable Model . *Phys. Rev. Lett.* 111:030602
- [34] Allahverdyan AE, Hovhannisyanyan KV, Melkikh AV, Gevorkian SG. 2013. Carnot cycle at finite power: Attainability of maximal efficiency. *Phys. Rev. Lett.* 111:050601
- [35] Boukobza E, Ritsch H. 2013. Breaking the carnot limit without violating the second law: A thermodynamic analysis of off-resonant quantum light generation. *Phys. Rev. A* 87:063845
- [36] Levy A, Alicki R, Kosloff R. 2012. Quantum refrigerators and the third law of thermodynamics. *Phys. Rev. E* 85:061126
- [37] Linden N, Popescu S, Skrzypczyk P. 2010. "how small can thermal machines be? towards the smallest possible refrigerato". *Phys. Rev. Lett.* 105:130401
- [38] Luis A, Correa Jose P, Palao GA, Alonso D. 2013. Performance bound for quantum absorption refrigerators . *Phys. Rev. E* 87:042131
- [39] Martinez EA, Paz JP. 2013. Dynamics and thermodynamics of linear quantum open systems. *Phys. Rev. Lett.* 110:130406
- [40] Calusius R. 1850. "Ueber Die Bewegende Kraft Der Wrme Und Die Gesetze, Welche Sich Daraus Fr Die Wrmelehre Selbst Ableiten Lassen". *Annalen der Physik* 79:68
- [41] Lindblad G. 1976. On the generators of quantum dynamical semigroups. *Comm. Math. Phys.* 48:119
- [42] Gorini V, Kossakowski A, Sudarshan E. 1976. Completely positive dynamical semigroups of n-level systems. *J. Math. Phys.* 17:821
- [43] Spohn H, Lebowitz J. 1979. Irreversible thermodynamics for quantum systems weakly coupled to thermal reservoirs. *Adv. Chem. Phys.* 38:109
- [44] Kosloff R, Ratner M. 1984. Beyond Linear Response: Lineshapes for Coupled Spins or Oscillators via Direct Calculation of Dissipated Power. *J. Chem. Phys.* 80:2352–2362
- [45] Davis EB. 1974. Markovian Master Equations. *Comm. Math. Phys.* 39:91–110
- [46] Geva E, Kosloff R, Skinner J. 1995. On the relaxation of a two-level system driven by a strong electromagnetic field. *J. Chem. Phys.* 102:8541–8561
- [47] Szczygielski K, Gelbwaser-Klimovsky D, Alicki R. 2013. Markovian master equation and thermodynamics of a two-level system in a strong laser field. *Phys. Rev. E* 87:012120
- [48] Gorini V, Kossakowski A. 1976. N-level system in contact with a singular reservoir. *J. Math. Phys.* 17:1298

- [49] C. Cohen-Tannoudji, J. A. Dupont-Roc, G. Grynberg. 1987. "Atom-Photon Interaction". Wiley
- [50] Lamb W. 1964. Theory of an Optical Maser. *Phys. Rev.* 134:1429
- [51] Louisell WH. 1990. *Quantum Statistical Properties of Radiation*. Wiley
- [52] Digonnet MJF. 1990. Closed-Form Expressions for the Gain in Three- and Four-Level Laser Fibers . *IEEE J. Quantum Electronics* 26:1788
- [53] Scully MO, Zubairy MS, Agarwal GS, Walther H. 2003. Extracting work from a single heat bath via vanishing quantum coherence. *Science* 299:862
- [54] Scully MO. 2010. Quantum photocell: Using quantum coherence to reduce radiative recombination and increase efficiency. *Phys. Rev. Lett.* 104:207701
- [55] Svidzinsky AA, Dorfman KE, Scully MO. 2011. Enhancing photovoltaic power by fano-induced coherence. *Phys. Rev. A* 84:053818
- [56] Scully MO, Chapin KR, Dorfman KE, Kim MB, Svidzinsky A. 2011. Quantum heat engine power can be increased by noise-induced coherence. *Proc. Natl. Acad. Sci. U S A* 108:15097
- [57] Harbola U, Rahav S, Mukamel S. 2012. Quantum heat engines: A thermodynamic analysis of power and efficiency. *Eur. Phys. Lett.* 99:50005
- [58] Rahav S, Harbola U, Mukamel S. 2012. Heat fluctuations and coherences in a quantum heat engines. *Phys. Rev. A* 86:043843
- [59] Goswami HP, Harbola U. 2013. Thermodynamics of quantum heat engines . *Phys. Rev. A* 88:013842
- [60] D. Gelbwaser-Klimovsky RA, Kurizki G. 2013. Minimal universal quantum heat machine. *Phys. Rev. E* 87:012140
- [61] Boukobza E, Tannor DJ. 2007. Three-level systems as amplifiers and attenuators: A thermodynamic analysis. *Phys. Rev. Lett.* 98:240601
- [62] Alicki R, Fannes M. 2013. Entanglement boost for extractable work from ensembles of quantum batteries . *Phys. Rev. E* 87:042123
- [63] Gelbwaser-Klimovsky D, Alicki R, Kurizki G. 2013. How much work can a quantum device extract from a heat engine? *ArXiv e-prints: 1302.3468*
- [64] Nernst W. 1906. Ueber die Berechnung chemischer Gleichgewichte aus thermischen Messungen. *Nachr. Kgl. Ges. Wiss. Gött.* 1:40
- [65] Nernst W. 1906. Über die Beziehung zwischen Wärmeentwicklung und maximaler Arbeit bei

- kondensierten Systemen. *er. Kgl. Pr. Akad. Wiss.* 52:933
- [66] Nernst W. 1918. *The theoretical and experimental bases of the New Heat Theorem Ger., Die theoretischen und experimentellen Grundlagen des neuen Wärmesatzes.* Halle: W. Knapp
- [67] Fowler RH, Guggenheim EA. 1939. *Statistical Thermodynamics.* Cambridge university press
- [68] Landsberg PT. 1989. A comment on nernst's theorem. *J. Phys A: Math.Gen.* 22:139
- [69] Belgiorno F. 2003. Notes on the third law of thermodynamics i. *J. Phys A: Math.Gen.* 36:8165
- [70] Belgiorno F. 2003. Notes on the third law of thermodynamics ii. *J. Phys A: Math.Gen.* 36:8195
- [71] Levy A, Alicki R, Kosloff R. 2012. Comment on Cooling by Heating: Refrigeration Powered by Photons". *Phys. Rev. Lett.* 109:248901
- [72] Geusic J, Bois E, De Grasse R, Scovil H. 1959. Three level spin refrigeration and maser action at 1500 mcsec. *J. App. Phys.* 30:1113
- [73] Tsujikawa I, Murao T. 1962. Possibility of Optical Cooling of Ruby. *J. Phys. Soc. Jpn.* 18:503
- [74] G. C. Dousmanis C. W. Mueller HN, Petzinger KG. 1964. Evidence of refrigerating action by means of photon emission in semiconductor diodes. *Phys. Rev.* 133:A316
- [75] Kushida T, Geusic JE. 1968. Optical refrigeration in nd-doped yttrium aluminum garnet. *Phys. Rev. Lett.* 20:1172
- [76] Wineland DJ, Dehmelt H. 1975. . *Bull. Am. Phys. Soc.* 20:637
- [77] Hänsch TW, Schawlow AL. 1975. Cooling of Gases by Laser Radiation. *Opt. Commun.* 13:368
- [78] Lett PD, Watts RN, Westbrook CI, Phillips WD, Gould PL, Metcalf HJ. 1988. Observation of atoms laser cooled below the doppler limit. *Phys. Rev. Lett.* 61:169
- [79] Shevy Y, Weiss DS, Ungar PJ, Chu S. 1989. Bimodal speed distributions in laser-cooled atoms . *Phys. Rev. Lett.* 62:1118
- [80] Dalibard J, Cohen-Tannoudji C. 1989. "Laser cooling below the Doppler limit by polarization gradients: simple theoretical models". *J. Opt. Soc. Am. B* 79:2023
- [81] Steck DA. 2003. Sodium D Line Data
steck.us/alkalidata/sodiumnumbers.1.6.pdf
- [82] Gordon JM, Ng KC. 2000. *Cool Thermodynamics.* Cambridge International Science Pub-

lishing

- [83] Einstein A, Szilárd L. 1930. "refrigeration". "US patent No 1,781,541"
- [84] Mari A, Eisert J. 2012. Cooling by heating: Very hot thermal light can significantly cool quantum systems. *Phys. Rev. Lett.* 108:120602
- [85] Cleuren B, Rutten B, Van den Broeck C. 2012. Cooling by Heating: Refrigeration Powered by Photons. *Phys. Rev. Lett.* 108:120603
- [86] Venturelli D, Fazio R, Giovannetti V. 2013. Minimal self-contained quantum refrigeration machine based on four quantum dots. *Phys. Rev. Lett.* 110:256801
- [87] Pekola JP, Hekking FWJ. 2007. Normal-Metal-Superconductor Tunnel Junction as a Brownian Refrigerator. *Phys. Rev. Lett.* 98:210604
- [88] Correa LA, Palao JP, Alonso D, Adesso G. 2013. Quantum-enhanced absorption refrigerators. *ArXiv e-prints:1308.4174*
- [89] Levy A, Kosloff R. 2012. Quantum absorption refrigerator. *Phys. Rev. Lett.* 108:070604
- [90] Skrzypczyk P Brunner N, Popescu S. 2011. "the smallest refrigerators can reach maximal efficiency". *J. Phys A: Math.Gen.* 44:492002
- [91] Brunner N, Linden N, Popescu S, Skrzypczyk P. 2012. "virtual qubits, virtual temperatures, and the foundations of thermodynamics". *Phys. Rev. E* 85:051117
- [92] Breuer HP, Petruccione F. 2002. *Open quantum systems*. Oxford university press
- [93] Łuczka J, Niemeic M. 1991. "a master equation for quantum systems driven by poisson white noise". *J. Phys A: Math.Gen.* 24:L1021
- [94] Alicki R, Lidar DA, Zanardi P. 2006. Internal consistency of fault-tolerant quantum error correction in light of rigorous derivations of the quantum Markovian limit . *Phys. Rev. A* 73:052311
- [95] Kolář M, Gelbwaser-Klimovsky D, Alicki R, Kurizki G. 2012. Quantum bath refrigeration towards absolute zero: unattainability principle challenged. *Phys. Rev. Lett.* 108:090601
- [96] Alhassid Y, Levine R. 1978. Exact conditions for the preservation of a canonical distribution in markovian relaxation processes. *Phys. Rev. A* 18:89
- [97] Kosloff R, Feldmann T. 2002. A Discrete Four Stroke Quantum Heat Engine Exploring the Origin of Friction. *Phys. Rev. E* 65:055102
- [98] Feldmann T, Kosloff R. 2003. The Quantum Four Stroke Heat Engine: Thermodynamic Observables in a Model with Intrinsic Friction. *Phys. Rev. E* 68:016101

- [99] Rezek Y, Kosloff R. 2006. Irreversible performance of a quantum harmonic heat engine. *New J. Phys.* 8:83
- [100] Ashkenazi G, Kosloff R and Ratner MA. 1999. Photoexcited electron transfer: Short-time dynamics and turnover control by dephasing, relaxation, and mixing. *J. Am. Chem. Soc.* 121:3386–3395
- [101] Bartana A, Kosloff R, Tannor DJ. 1993. Laser Cooling of Molecular Internal Degrees of Freedom by a Series of Shaped Pulses. *J. Chem. Phys.* 99:196–210
- [102] Wu L., Segal D. and Brumer P. 2013. No-go theorem for ground state cooling given initial system-thermal bath factorization . *Sci Rep.* 3:1824
- [103] Skrzypczyk P, Short AJ, Popescu S. 2013. Extracting work from quantum systems. *ArXiv e-prints: 1302.2811*
- [104] Hovhannisyan KV, Perarnau-Llobet M, Huber M, Acín A. 2013. The role of entanglement in work extraction. *ArXiv e-prints:1303.4686*
- [105] Brunner N, Huber M, Linden N, Popescu S, Silva R, Skrzypczyk P. 2013. Entanglement enhances performance in microscopic quantum fridges. *ArXiv e-prints: 1305.6009*
- [106] Geva E, Kosloff R. 1992. A Quantum Mechanical Heat Engine Operating in Finite Time. A Model Consisting of Spin *half* Systems as The Working Fluid. *J. Chem. Phys.* 96:3054–3067
- [107] Geva E, Kosloff R. 1992. On the Classical Limit of Quantum Thermodynamics in Finite Time. *J. Chem. Phys.* 97:4398–4412
- [108] Feldmann T, Geva E, Kosloff R, Salamon P. 1996. Heat Engines in Finite Time Governed by Master Equations. *Am. J. Phys.* 64:485–492
- [109] He JiZhou HX, Wei T. 2009. "the performance characteristics of an irreversible quantum otto harmonic refrigeration cycle". *Science in China Series G-Phys. Mech. & Ast.* 52:1317
- [110] Wang H. 2013. Quantum-mechanical brayton engine working with a particle in a one-dimensional harmonic trap. *Physica Scripta* 87:055009
- [111] Wang R, Wang J, He J, Ma Y. 2013. Efficiency at maximum power of a heat engine working with a two-level atomic system . *Phys. Rev. E* 87:042119